LARGE-SCALE BIOLOGY ARTICLE

Multiplex CRISPR-Cas9 editing of DNA methyltransferases in rice uncovers a class of non-CG methylation specific for GC-rich regions

Daoheng Hu[1,2,*], Yiming Yu[1,*], Chun Wang[3,*], Yanping Long[1], Yue Liu[1], Li Feng[1], Dongdong Lu[1], Bo Liu[1], Jinbu Jia[1], Rui Xia[2], Jiamu Du[1], Xuehua Zhong[4], Lei Gong[5], Kejian Wang[3,†] and Jixian Zhai[1,†]

[1] School of Life Sciences & Institute of Plant and Food Science & Key Laboratory of Molecular Design for Plant Cell Factory of Guangdong Higher Education Institutes, Southern University of Science and Technology, Shenzhen, Guangdong 518055, China;

[2] College of Horticulture, South China Agricultural University, Guangzhou, 510642, China;

[3] State Key Laboratory of Rice Biology, China National Rice Research Institute, Chinese Academy of Agricultural Sciences, Hangzhou, China;

[4] Laboratory of Genetics & Wisconsin Institute for Discovery, University of Wisconsin-Madison, Madison, WI, USA;

[5] Key Laboratory of Molecular Epigenetics of the Ministry of Education, Northeast Normal University, Changchun, 130024, China;

[*] These authors contributed equally to this work

[†] Correspondence: zhaijx@sustech.edu.cn (J.Z.) or wangkejian@caas.cn (K.W.)

Short title: The non-CG methylation landscape in rice

One-sentence summary: Examination of knockout mutants reveals that rice methyltransferases have subfunctionalized to accommodate a distinct cluster of non-CG methylated sites at highly GC-rich regions in the rice genome.

The author responsible for distribution of materials integral to the findings presented in this article in accordance with the policy described in the Instructions for Authors (www.plantcell.org) is: Jixian Zhai (zhaijx@sustech.edu.cn).

ABSTRACT

DNA methylation in the non-CG context is widespread in the plant kingdom and abundant in mammalian tissues such as the brain and pluripotent cells. Non-CG methylation in *Arabidopsis thaliana* is coordinately regulated by DOMAINS REARRANGED METHYLTRANSFERASE (DRM) and CHROMOMETHYLASE (CMT) proteins but has yet to be systematically studied in major crops due to difficulties in obtaining genetic materials. Here, utilizing the highly efficient multiplex CRISPR-Cas9 genome-editing system, we created single- and multiple-knockout mutants for all nine DNA methyltransferases in rice (*Oryza sativa*) and profiled their whole-genome

methylation status at single-nucleotide resolution. Surprisingly, the simultaneous loss of DRM2, CMT2, and CMT3 functions, which completely erases all non-CG methylation in Arabidopsis, only partially reduced it in rice. The regions that remained heavily methylated in non-CG contexts in the rice *Os-dcc* (*Osdrm2*/*cmt2*/*cmt3a*) triple mutant had high GC contents. Furthermore, the residual non-CG methylation in the *Os-dcc* mutant was eliminated in the *Os-ddccc* (*Osdrm2*/*drm3*/*cmt2*/*cmt3a*/*cmt3b*) quintuple mutant but retained in the *Os-ddcc* (*Osdrm2*/*drm3*/*cmt2*/*cmt3a*) quadruple mutant, demonstrating that OsCMT3b maintains non-CG methylation in the absence of other major methyltransferases. Our results showed that OsCMT3b is subfunctionalized to accommodate a distinct cluster of non-CG methylated sites at highly GC-rich regions in the rice genome.

Key words: non-CG methylation; DNA methyltransferase; OsCMT3b; *Oryza sativa*

INTRODUCTION

In plants, DNA methylation occurs in three sequence contexts, namely, CG, CHG, and CHH (where H denotes A, T, or C), and each context is established and maintained by distinct DNA methyltransferase families (Law and Jacobsen, 2010; He et al., 2011; Matzke and Mosher, 2014; Du et al., 2015; Zhang et al., 2018). In mammals, DNA methylation occurs predominantly in the CG context, and the non-CG methylation is only abundant in specific tissues such as the brain and pluripotent cells (He and Ecker, 2015). Recently, non-CG methylation has been found in specific cell-types in humans and mice (Lister et al., 2009; Xie et al., 2012), and may play important roles during differentiation (Schultz et al., 2015). In *Arabidopsis thaliana*, CG methylation is maintained by DNA METHYLTRANSFERASE 1 (MET1) (Ronemus et al., 1996); CHG methylation is maintained by CHROMOMETHYLASE3 (CMT3) with the help of the H3K9 histone methyltransferase KRYPTONITE/SUVH4 (KYP) (Cao and Jacobsen, 2002; Du et al.,

2012); and CHH methylation is established and maintained by DOMAINS REARRANGED METHYLTRANSFERASE2 (DRM2) through RNA-directed DNA methylation, as well as by CMT2 and DECREASE IN DNA METHYLATION1 (DDM1) in a small interfering RNA-independent manner (Cao et al., 2003; Lister et al., 2008; Stroud et al., 2013a; Zemach et al., 2013; Stroud et al., 2014).

The rice (*Oryza sativa*) genome encodes nine putative DNA methyltransferases, with two copies of MET, three CMTs, and four DRMs (Sharma et al., 2009). Previous studies have shown that OsMET1b is the major CG methylase and that the *Osmet1b* homozygous mutant has severe developmental defects that lead to seedling lethality (Hu et al., 2014; Yamauchi et al., 2014), whereas the *Osmet1a* mutant did not show an obvious developmental defect (Yamauchi et al., 2009). OsCMT3a was shown to mediate CHG methylation, and *Oscmt3a* mutants exhibited pleiotropic developmental abnormalities as well as activation of a wide spectrum of transposons (Cheng et al., 2015). OsDRM2 is required for *de novo* DNA methylation and is critical for both vegetative and reproductive growth (Moritoh et al., 2012), and the *Osdrm2* mutant exhibits drastically reduced CHH methylation.

Due to the difficulties in obtaining higher-order mutants, cooperation between different DNA methyltransferases has yet to be explored in rice. However, in the last few years, exciting developments in CRISPR-Cas-based genome-editing technology have fundamentally reshaped functional genomics in all organisms, including plants (Li et al., 2017b; Knott and Doudna, 2018; Chen et al., 2019). The technology is particularly groundbreaking in rice due to the high efficiency of the CRISPR-Cas9 system in rice calli during transformation (Wang et al., 2015), with many homozygous and heterozygous

single- and multiple-knockout mutants readily obtained in the T0 generation. Here, taking advantage of this highly efficient system, we extensively investigated the non-CG DNA methylation landscape in rice.

RESULTS

Multiplexed knockouts of DNA methyltransferases via CRISPR-Cas9 in rice

To systemically examine all nine DNA methyltransferases and investigate the coordination among non-CG methyltransferases, we took advantage of the multiplex CRISPR-Cas9 genome-editing tool to target each of the nine DNA methyltransferase genes individually as well as using single-guide RNA (sgRNA) combinations to simultaneously target multiple non-CG methyltransferases (Figure 1A; Supplemental Table S1). In total, nine single-knockout constructs, five double-knockout constructs, one triple-knockout construct, and one quintuple-knockout construct were used for rice transformation (Supplemental Table S2). Subsequently, we screened a large number of Cas9-positive T1 plants using a high-throughput, next-generation sequencing-based method (Liu et al., 2019) and obtained homozygous mutants carrying frameshifting insertions or deletions for all sixteen of the desired genotypes except *Osmet1b*, which was previously reported to be seedling lethal (Hu et al., 2014) (Figure 1B; Supplemental Figures S1 and S2).

Phenotypes of the CRISPR-Cas9-derived single mutants were consistent with those previously described for single mutants generated using T-DNA or Tos17 transposition (Moritoh et al., 2012; Cheng et al., 2015; Tan et al., 2016), with *Osdrm2* displaying severe developmental defects and *Oscmt3a* being sterile. Simultaneous loss of multiple

non-CG DNA methyltransferases further enhances the developmental defects observed in *Osdrm2*, suggesting non-CG methylation plays a major role in regulating vegetative and reproductive development (Figure 1C; Supplemental Figure S3). It is worth noting that, although the highly efficient CRISPR system in rice enables us to obtain a large number of single, double, and higher-order mutants in a relatively short period of time compared to the traditional T-DNA-based method combined with crossing, the downside is that each individual mutant line is derived from independent transformation events and therefore may carry different mutant alleles for the same gene, and the frameshifting mutants, despite typically being null alleles, might still be partially functional.

Osdrm2/cmt2/cmt3a **triple mutant reveals the cooperative regulation of CHH methylation in rice**

Next, we characterized the impacts of these mutants on DNA methylation at single-base pair resolution using whole-genome bisulfite sequencing (WGBS; Figure 1B; Supplemental Data Set S1). To track possible epigenetic changes caused by tissue culture (Stroud et al., 2013b), both nontransformed Nipponbare and segregated wild-type T1 plants that underwent the transformation process were examined as controls. By comparing genome-wide methylation statuses from different libraries to identify differentially methylated regions (DMRs, see the “Methods” and “Accession Numbers” sections for more details), we found that CHG methylation was largely lost in *Oscmt3a*, with a small subset of loci specifically demethylated in *Osdrm2* (Figure 2A, C-D). Meanwhile, the majority of CHH methylation was eliminated in *Osdrm2* mutants, with OsCMT2 and OsCMT3a playing minor roles in a small percentage of the genome (Figure

2B, F-H). The single mutants of *OsDRM1a*, *OsDRM1b*, *OsDRM3*, and *OsCMT3b* globally did not show visible losses of CHG or CHH methylation (Figure 2A-B), but each has a small number of non-CG hypo-DMRs (Supplemental Data Set S1), enriched over subgroups of transposable elements (TEs; Supplemental Figure S4). Hence, OsCMT2, OsCMT3a, and OsDRM2 are the three major players in the maintenance of non-CG methylation in rice.

To further explore the coordination among the three major non-CG DNA methyltransferases in rice, we investigated the impacts of their combinatorial mutants, including all the double (*Osdrm2*/*cmt2*, *Osdrm2*/*cmt3a*, and *Oscmt2*/*cmt3a*) and triple (*Os-dcc*) mutants. We found that *Osdrm2*/*cmt3a* double mutants had a greater loss of CHG methylation than either the *Oscmt3a* or *Osdrm2* single mutant (Figure 2A, E), suggesting that OsCMT3a and OsDRM2 cooperate in methylating CHG contexts in specific genomic regions. Unexpectedly, few CHG DMRs were found in the *Oscmt2* single mutant, and almost all the *Os-dcc* CHG DMRs overlapped with *Osdrm2*/*cmt3a* CHG DMRs (Figure 2A, C-E). Hence, in contrast to the case in Arabidopsis, in which CMT2 contributes to CHG methylation (Stroud et al., 2014), OsCMT3a and OsDRM2 (but not OsCMT2) are responsible for most of the CHG methylation in rice.

In Arabidopsis, *cmt3* CHH DMRs are a small subset of *cmt2* CHH DMRs, and *drm2*/*cmt2* erases all CHH methylation (Stroud et al., 2014). By comparing *Osdrm2*/*cmt2* and *Os-dcc* mutants, we found that a large number of CHH DMRs were controlled by OsCMT3a alone (Figure 2B). Furthermore, the CHH DMRs found in either the *Oscmt2* or *Oscmt3a* single mutant exhibited additional loss of methylation in the *Oscmt2*/*cmt3a* double mutant (Figures 2I; Supplemental Figure S5A-B), suggesting functional

redundancy between these two enzymes. However, *Osdrm2* CHH DMRs showed no loss of methylation in the *Oscmt2*, *Oscmt3a*, and *Oscmt2*/*cmt3a* mutants (Figure 2F; Supplemental Figure S5C), suggesting that targets of OsDRM2 were insulated from the activity of OsCMT2/CMT3a. A previous study on the subtype of CHG and CHH sites in Arabidopsis, maize (*Zea mays*), and tomato (*Solanum lycopersicum*) revealed that the differential methylation in the CHG and CHH subcontexts is affected by properties of the DNA methylation machinery (Gouil and Baulcombe, 2016). From these results, we conclude that CMT2 plays a much weaker role in rice than in Arabidopsis and that OsCMT3a is capable of methylating the CHH context in the rice genome.

Non-CG methyltransferases coordinately regulate the transcriptome

Next, we examined the impacts of these mutants on the transcriptome using RNA-seq (Figure 1B) to look for TEs with significantly altered expression levels (at least four-fold change and an adjusted p-value < 0.01) (Stroud et al., 2013b). We found that in general, the double mutants had a larger number of upregulated TEs than the single mutants, with the largest number observed in the *Os-dcc* triple mutant (Figure 2J; Supplemental Data Set S3). A similar trend was observed for genic regions, with the largest number of differentially expressed genes also reported in *Os-dcc* (Supplemental Figure S6A; Supplemental Data Set S3). In addition to the number of loci affected, the change in expression level for the same set of upregulated TEs/genes was also the most prevalent in the *Os-dcc* triple mutant (Figure 2K; Supplemental Figure S6B). *Oscmt3a* had a larger number of upregulated TEs than *Osdrm2* and *Oscmt2*, suggesting that CHG methylation plays a greater role in silencing TEs than CHH methylation does (Figure 2J). These data

suggest that OsDRM2, OsCMT2, and OsCMT3a coordinately regulate the transcription of TEs and genes.

Furthermore, we analyzed the methylation levels of upregulated and downregulated TEs identified from a series of mutants, and found that upregulated TEs in general are with significantly higher levels of CHG methylation compared to downregulated ones (Supplemental Figure S6D). The regions of methylation cover the entire body of TEs including upstream and downstream (Supplemental Figure S6E). The higher CHG level of upregulated TEs might be related to the greater drop in CHG methylation of these regions in the mutants, as most TEs lost all CHG methylation in the mutants (Supplemental Figure S6F).

Small RNAs are important regulatory molecules in plant development, environmental response, and genome defense (Borges and Martienssen, 2015; Song et al., 2019). Some 24-nt small interfering RNAs (siRNAs) are trigger molecules for RNA-directed DNA methylation (RdDM), and their precursors are produced by plant-specific RNA polymerase IV (Pol IV), which can transcribe silent TE regions (Matzke and Mosher, 2014). Pol IV targeting requires DNA methylation, and the production of 24-nt siRNAs is drastically reduced in Arabidopsis *drm2* hypo-CHH DMRs (Stroud et al., 2014). We checked the relationship between non-CG methylation and 24-nt siRNA accumulation in the rice mutants (Figure 2L). We analyzed the 24-nt siRNAs mapped to the *Os-dcc* CHG and CHH DMRs and found that most of the siRNAs were lost in the *Osdrm2* single mutant (Figure 2L), suggesting that OsDRM2-dependent CHH and CHG methylation are required for Pol IV siRNA biogenesis. In contrast to the case in Arabidopsis, in which 24-nt siRNAs in *cmt2* CHH DMRs are mostly independent of

DRM2 activity (Stroud et al., 2014), the 24nt-siRNAs at *Oscmt2* CHH hypo-DMRs are only lost in the *Osdrm2* mutant but not *Oscmt2* or *Oscmt3a* (Supplemental Figure S6C), consistent with a stronger role of DRM2 in methylating CHH context in this species.

The residual non-CG methylation in *Os-dcc* features a high GC content and is lost in *Os-ddccc* quintuple mutants

The most striking observation in the *Os-dcc* triple mutant was the high level of residual non-CG methylation (Figures 2A-B, and 3A-B). The Arabidopsis *ddcc* (*drm1*/*drm2*/*cmt2*/*cmt3*) mutant is essentially equivalent to the *drm2*/*cmt2*/*cmt3* triple mutant because *DRM1* is transcribed only in the mature egg cell of Arabidopsis (Jullien et al., 2012). Our WGBS data on *Osdrm1a*, *Osdrm1b*, and the *Osdrm1a*/*drm1b* double mutants also revealed no change in their DNA methylation patterns (Figure 2A-B), consistent with the limited role of DRM1 in somatic tissues. However, in contrast to the complete loss of all non-CG methylation in the Arabidopsis *ddcc* mutant (Stroud et al., 2014), 5% of all mCHG sites and 23% of the mCHH sites remain methylated in the *Os-dcc* mutant (Figure 3A). These regions with residual methylation in *Os-dcc* mostly retained both CHG and CHH methylation (Figure 3B; Supplemental Figure S7A-B), and the expression level of genes and TEs in these regions are generally lower than the whole-genome average (Figure 4A-B). They also produce less 24-nt siRNAs (Figure 4C).

Compared to the average level across the genome, regions that remain methylated in *Os-dcc* are depleted of SINE, LINE, and MITE TEs, but have a much higher portion of the CACTA transposons and LTR-Retrotransposons (Figure 4D), and these regions are enriched in TEs and lack genes (Figure 4E). This could be due to the fact that CACTA

transposons and LTR-Retrotransposons are largely located in heterochromatic regions, where small RNAs are largely depleted compared to RdDM sites (Stroud et al., 2014). Publicly available ChIP-seq data showed that these regions have the typical modifications at TE-rich heterochromatic chromatin, being enriched with H3K9me2, low in active genic marks such as H3K27ac, H3K4me3, H3K36me3, and having relatively low levels of H3K27me3 (Figure 4F, G). GO enrichment analysis on genes located at the regions did not find GO terms that are significantly enriched (Supplemental Tables S3 and S4).

Despite having no obvious correlation with common histone modifications or small RNA accumulation (Figure 4C, F-G), a detailed examination of several loci suggested a possible connection to GC content, as these regions are often highly GC-rich (Figure 3B). Next, we examined the level of non-CG methylation against GC content using wild-type data from rice and Arabidopsis, and all the bins are a fixed length of 200 bp. It was immediately clear that the rice methylome features two distinct branches of methylated regions in both CHG and CHH contexts, one with medium GC content (~0.4) and the other with high GC content (0.6 ~ 0.8) (Figure 3C-D), whereas Arabidopsis has only a medium GC content branch (Figure 3E-F), probably due to the fact that fewer TEs exist in the Arabidopsis genome compared to rice (Yu et al., 2002), and TEs are the major targets of DNA methylation.

The two branches of mCHH and mCHG sites in rice behave drastically differently in various mutants. The medium GC content branch lost almost all of the CHG methylation in *Oscmt3a* and *Os-dcc* and showed severe loss of CHH methylation in the *Osdrm2* and *Os-dcc* triple mutant (Figure 3C-D), patterns resembling the medium GC content branch in the Arabidopsis WT and *ddcc* mutant (Figure 3E-F). In contrast, the high GC content

branch retained a majority of the CHG and CHH methylation in all the single, double, or even *Os-dcc* triple mutants but lost most non-CG methylation in the *Os-ddccc* quintuple mutant (Figure 3C-D). Consistent with these results, the remaining mCHG and mCHH sites in *Os-dcc* were also exclusively found in the highly GC-rich regions (Supplemental Figure S8A-B). Thus we have identified two distinct classes of regions in rice based on GC content: medium GC content regions that are dependent on the function of the three major methylases CMT2/CMT3/DRM2 and also found in Arabidopsis, as well as a group of highly GC-rich regions that are subject to methylation by minor DNA methyltransferases in the *Os-dcc* triple mutant and lost methylation in the *Os-ddccc* quintuple mutant.

The GC-rich cluster of non-CG methylated sites is distinct in rice and methylated by OsCMT3b

Widespread variation of DNA methylation patterns has been reported in angiosperms (Niederhuth et al., 2016). GC content is predicted to have major impacts on genome functioning and ecological adaptation, and GC-rich DNA could potentially facilitate more complex gene regulation (Smarda et al., 2014). Moreover, rice and maize genomes contain a separate group of extremely GC-rich genes that are absent in Arabidopsis, whose genes are mostly AT-rich (Tatarinova et al., 2010). Given that the highly GC-rich branch of mCHG and mCHH sites was found in the rice genome but not in the Arabidopsis genome, we next examined if this branch exists in other plant species.

Recent developments in genome sequencing and assembly have led to the accumulation of many high-quality plant genomes with WGBS data, and we analyzed the

277 correlation between DNA methylation and GC content in five additional plant species
278 (see the "Methods" section for more details). We found that the *Brachypodium*
279 *distachyon* and maize (B73 and Mo17) genomes contain a relatively GC-rich branch of
280 mCHG sites, consistent with the well-known observation of bimodal GC content in
281 monocots (Tatarinova et al., 2010), but no clear GC-rich branch was observed for mCHH
282 sites (Figure 5A-B). For *Sorghum bicolor*, soybean (*Glycine max*), and tomato, we did
283 not observe the GC-rich branch for either mCHG or mCHH sites, resembling patterns
284 observed in Arabidopsis (Figures 5A-B, and 3E-F). Hence, the highly GC-rich cluster of
285 non-CG methylated sites seems to be unique for the rice genome.

286 To further investigate whether OsCMT3b or OsDRM3 maintains the non-CG
287 methylation at GC-rich regions of *Os-dcc* triple mutant, we performed an analysis of non-
288 CG methylation level of DMRs between the *Os-dcc* triple mutant and *Os-ddccc* quintuple
289 mutant (Supplemental Data Set S2), and examined the methylation status of these DMRs
290 in *Os-dcc*, *Os-ddcc* (*Osdrm2/drm3/cmt2/cmt3a*), and *Os-ddccc*. We found the non-CG
291 methylation level of DMRs between the *Os-dcc* triple mutant and *Os-ddccc* quintuple
292 mutant are similar between *Os-ddcc* quadruple mutant and *Os-dcc* triple mutant (Figure
293 5C-D). This suggests that OsCMT3b can maintain the non-CG methylation at GC-rich
294 regions of *Os-dcc* triple mutant.

295 OsCMT3b was categorized as a member of the ZMET group, which is a monocot-
296 specific group (Bewick et al., 2017). In *Z. mays*, ZMET2 contributes to the maintenance
297 of most mCHG and a part of mCHH within some loci, whereas, ZmMET5, a paralog of
298 ZMET2, catalyzes the maintenance of mCHG to a lesser degree (Li et al., 2014).
299 OsCMT3a and OsCMT3b, the orthologs of ZMET2 and ZMET5, were identified as dual-

functional DNA methyltransferases that can maintain both mCHG and mCHH (Figure 2A-B; Supplemental Figure S9A-B). Compared with the more similar ZMET2 and ZMET5 pair, OsCMT3b shows much more divergence with its paralogous OsCMT3a (Supplemental Figure S10), suggesting possible subfunctionalization. OsCMT3b can maintain the non-CG methylation at GC-rich regions of *Os-dcc* triple mutant, whereas the *Oscmt3b* mutant does not show DNA methylation defect (Figure 2A-B; Figure 5C-D). Comparisons of non-CG DMRs from *Oscmt3a* vs *Oscmt3b*, as well as those from *Os-ddcc* vs *Os-ddccc* also illustrated that loss of OsCMT3b function has a much greater impact on non-CG methylation in the *Os-ddcc* background than in the WT background (Supplemental Figure S9). This suggests that an alternative mechanism to maintain the non-CG methylation at GC-rich regions exists in rice when the major non-CG methyltransferases are defective, and these non-CG methylations are catalyzed by OsCMT3b. The residual non-CG methylation in *Os-dcc*, which was targeted by OsCMT3b, can alleviate part of the growth defects of *Os-ddccc* (Figure 1C).

DISCUSSION

A recent study showed that specific variant forms of the CHG and CHH contexts could be preferentially targeted by different DNA methylation pathways in Arabidopsis, maize, and tomato (Gouil and Baulcombe, 2016). Our collection of mutants in rice provides an opportunity to compare the impacts of mutating *OsDRM2*, *OsCMT2*, and *OsCMT3*a on the different mCHG or mCHH contexts by looking at their representation at *Os-dcc* DMRs. Consistent with a previous study (Gouil and Baulcombe, 2016), we found that mCCG has the lowest level of methylation at *Os-dcc* CHG hypo-DMRs; meanwhile, at

CHH hypo-DMRs, *Osdrm2* have the strongest impacts on the CAA, CAT, CTA sites (Supplemental Figure S11A-B), possibly reflecting its role on the relatively low GC content regions in rice. The wide range of CMT2 functionality among different plants is fascinating, while a majority of CHH methylation sites in Arabidopsis are mediated by AtCMT2 (Zemach et al., 2013; Stroud et al., 2014), OsCMT2 has a much more limited role in rice, and the maize genome is lacking a CMT2 ortholog (Zemach et al., 2013; Li et al., 2014; Gouil and Baulcombe, 2016). Despite having no CMT2, CAA and CTA are still the preferential CHH in maize genome as in Arabidopsis, and the two CMT3 orthologs in maize, Zmet2 and Zmet5, can catalyze both CHG and CHH methylation (Li et al., 2014; Gouil and Baulcombe, 2016). Future biochemical and structural characterization would be informative to further review the diverse substrate preference for plant DNA methyltransferases.

In Arabidopsis, the DRM3 lacks a conserved proline-cysteine in motif IV, which is essential for catalytic activity (Bestor and Verdine, 1994; Henderson et al., 2010; Zhong et al., 2015). Although OsDRM3 possesses a catalytic cysteine in motif IV, it lacks a preceding proline that promotes specific recognition and stabilizes the interaction between the base and catalytic site, and therefore is predicted to be catalytically inactive (Bestor and Verdine, 1994; Henderson et al., 2010). The catalytically inactive AtDRM3 acts to stimulate the activity of catalytic partner AtDRM2 at the step of catalysis, and is a general factor that has moderate effects on DNA methylation at RdDM targets (Henderson et al., 2010; Zhong et al., 2015). Similar to Arabidopsis, most CHH DRMs of *Osdrm3* have overlapped with *Osdrm2* CHH DMRs and the effect of the *Osdrm2* mutation was much stronger than *Osdrm3* mutation even at *Osdrm3* CHH DMRs

(Supplemental Figure S12A-C) (Zhong et al., 2015), suggesting that OsDRM3 shares similar mechanism with AtDRM3.

We also found that *Os-dcc* and *Os-ddcc* mutant share similar residual non-CG methylation at GC-rich branch; this suggests that OsDRM3 alone cannot maintain the residual non-CG methylation in *Os-dcc* mutant. Furthermore, the *Osdrm3* CHH DMRs are much less than *Atdrm3* CHH DMRs, suggesting OsDRM3 plays a much weak role in rice than AtDRM3 in Arabidopsis (Supplemental Figure S12A) (Zhong et al., 2015). Taking these results together, we speculate OsDRM3 may not be directly responsible for the residual non-CG methylation in *Os-dcc* mutants, and the other candidate OsCMT3b may maintain the residual non-CG methylation in *Os-dcc* mutant.

To directly investigate sites that are the putative targets of OsCMT3b and/or OsDRM3, we analyzed the DMRs between the *Os-dcc* triple mutant and *Os-ddccc* quintuple mutant (Supplemental Data Set S2), and found these DMRs largely overlap and therefore have similar features with those sites that remain methylated in the *Os-dcc* mutant in terms of Gene/TE expression pattern, chromosomal context, TE composition, distribution of 24-nt siRNAs (Supplemental Figure S13A-E); and these DMRs are also featured with high GC content (Supplemental Figure S13F, G).

While plants generally have low CHH methylation levels across the genome, methylation can reach high levels regionally, particularly for regions targeted by RdDM. Previous studies have discovered short regions of very high CHH methylation in maize, such as the mCHH islands located predominantly in more euchromatic regions and often near genes (Li et al., 2015), whose methylation requires ZmAGO4 and ZmDDM1 (Long et al., 2021). It is still unclear how the highly GC-rich regions are selectively targeted for

methylation in *Os-dcc*, we speculate that various locus-specific and context-sensitive methyl-CpG-binding domain proteins (Lang et al., 2015; Li et al., 2017a) and chromatin remodeling factors (Zhou et al., 2018) might be involved in facilitating the recruitment of DNA methylation machinery to the GC-rich regions in rice. For example, MBD7 was shown to prefer genomic regions with a high density of CG methylation (Lang et al., 2015).

In summary, we performed a comprehensive investigation of DNA methyltransferases in rice and discovered that there is a distinct cluster of non-CG methylated sites with high GC-content that remain methylated in the *Osdrm2*/*cmt2*/*cmt3a* triple mutant. These sites are targeted by OsCMT3b as their methylation is maintained in *Osdrm2*/*drm3*/*cmt2*/*cmt3a* quadruple mutants but is lost in the *Osdrm2*/*drm3*/*cmt2*/*cmt3a*/*cmt3b* quintuple mutants. Our results showed that the OsCMT3b in rice has evolved to accommodate the high GC content and maintain non-CG methylation in high-C density regions.

MATERIALS AND METHODS

Vector construction

The genome-editing vectors containing the CRISPR-Cas9 system were constructed via the isocaudomer ligation method as described previously (Wang et al., 2015). The modified single-guide RNA (sgRNA) scaffold and *ACTIN1* promoter-driven Cas9 were used to increase the efficiency of genome editing in this research (Hu et al., 2018). First, each of the double-stranded target oligonucleotides (Supplemental Table S1) was ligated into the SK-sgRNA vector digested with *AarI*. Then, based on anticipated mutant types,

some of these sgRNAs were assembled into one pC1300-ACT:Cas9 binary vector, using T4 ligase, to obtain the CRISPR-Cas9 vectors (Supplemental Table S2) for the generation of various DNA methyltransferase mutants.

Plant materials and transformation

Rice (*Oryza sativa* L. ssp. *japonica* 'Nipponbare') plants were used as the host in this study. The generation of transgenic rice by *Agrobacterium*-mediated transformation with strain EHA105 was performed by Hangzhou Biogle Co., Ltd. (Hangzhou, China). The seeds of T0 mutants and the callus culture-regenerated wild type were germinated and grown in hormone-free ½-strength Murashige and Skoog medium under 14/10 h of light (PHILIPS SON-T Argo (10,000 Lux)/dark at 28℃/25℃ in a growth chamber for 21 days. Then, the seedlings of homozygous T1 mutants were transplanted in the greenhouse and grown in the mud under 14/10 h of light (PHILIPS SON-T Argo 20,000 Lux)/dark at 34℃/25℃. Mature leaves of 70-day-old plants of each genotype were harvested for genomic DNA and total RNA extraction.

Genotyping of DNA methyltransferase mutations

Hi-TOM (high-throughput tracking of mutations), which is particularly suitable for high-throughput identification of all types of mutations induced by CRISPR-Cas systems(Liu et al., 2019), was used to genotype the T0 plants and the progenies of T0 mutants. The homozygous mutants of T0 and T1 plants identified by Hi-TOM were verified by Sanger sequencing. The primers used for genotyping are listed in Supplemental Table S5.

WGBS library construction, sequencing, and analysis

Genomic DNA was extracted from the mature leaves of 70-day-old wild-type and mutant plants using a DNeasy Plant Mini Kit (Qiagen). The libraries were prepared and sequenced at the GENEWIZ Bioinformatics Institute on the Illumina HiSeq X Ten platform. In brief, for library construction, 1 μg genomic DNA was fragmented to ~500 bp by sonication (Covaris S220), then treated with End Prep Enzyme Mix for end repairing, 5' Phosphorylation and dA-tailing in one reaction (Vazyme dA-Tailing Enzyme Mix, NR602-02-AI), followed by a T-A ligation to add Methylated adaptors to both ends (Vazyme VAHTS Universal Adapter Ligation Module for Illumina, N204-02). Size selection of Adaptor-ligated DNA was then performed using VAHTS DNA Clean Beads (Vazyme), and fragments of ~410 bp (with the approximate insert size of 350 bp) were recovered and followed by bisulfite conversion using EZ DNA Methylation-Lightning Kit (ZYMO).

We used public WGBS data for the *Arabidopsis thaliana* wild type (GSM1242401) and *ddcc* mutant (GSM1242404) (Stroud et al., 2014), *Brachypodium distachyon* (GSM2096945) (Niederhuth et al., 2016), *Zea mays* (SRP022569) (Eichten et al., 2013), *Sorghum bicolor* (GSM1821507) (Turco et al., 2017), *Glycine max* (GSM1008196) (Lin et al., 2017) and *Solanum lycopersicum* (SRX2008738) (Gouil and Baulcombe, 2016). High-quality reference genomes of rice (MSU7.0) (Kawahara et al., 2013), Arabidopsis (TAIR10) (Huala et al., 2001), Brachypodium (Brachypodium distachyon_v3.0) (Vogel et al., 2010), maize (B73 RefGen_v4) (Jiao et al., 2017), sorghum (Sorghum bicolor_v3) (McCormick et al., 2018), soybean (Wm82.a2.v1) (Song et al., 2016) and tomato (SL3.0) (Shearer et al., 2014) were used.

For each library, > 10 Gb of raw data was generated (Supplemental Data Set S1). Adapters were removed from reads using Cutadapt (Martin, 2011) v1.18, and the reads were then mapped to the reference genome using BSMAP (Xi and Li, 2009) v2.90, allowing 8% mismatches. DMRs were defined by comparing the DNA methylation levels between the wild type and each mutant in 200 bp bins, and were analyzed as previously described (Stroud et al., 2013b). The DNA methylation level in each 200bp bin was calculated based on read count by comparing the number of methylated cytosines with the total number of cytosines in all reads, calculated as #C/(#C+#T) (weighted methylation) (Schultz et al., 2012). In brief, DMRs were identified by Fisher's exact test with default parameters in the R package methylKit (Akalin et al., 2012) v1.9.3 with the criteria of an adjusted $P < 0.01$ and an absolute methylation difference of 0.7, 0.5, and 0.1 for the CG, CHG and CHH contexts, respectively (0.4, 0.2, and 0.1 for the CG, CHG and CHH contexts for Arabidopsis), between all wild types and mutants. Only bins that contained at least 4 informative cytosines (covered by at least 4 reads) in all wide types and mutants were retained as true DMRs. In Figure 2, the heatmap shows the methylation status of all 200 bp bins that have passed the DMR filter. All bins analyzed are of equal size, and we only merged adjacent bins for clustering DMRs to organize rows in the heatmap figures (Figure 2A-B), so that those 200bp bins that are derived from the same "merged DMR" stay together in the heatmap demonstration (for example, a single 1kb merged DMR would be displayed as five continuous 200bp bins). To define methylated CHG (mCHG) and methylated CHH (mCHH) sites, we used the same 200bp bins with DMR analysis, and filtered first in the WT/Control library for bins that have a methylation level no less than 0.7 for CG context, no less than 0.5 for CHG, and no less

than 0.1 for CHH, except for Arabidopsis with methylation level no less than 0.4 for CG, no less than 0.2 for CHG, and no less than 0.1 for CHH, respectively. The mCHG and mCHH sites were identified by the same way in *OS-dcc*/*ddccc* mutants of rice or *ddcc* mutants of Arabidopsis. So, the minimum methylation level of mCHG sites in the Control sample would be 0.5, and the minimum methylation level of mCHH sites would be 0.1 for the density plots, respectively (Figure 3C-D).

mRNA library construction, sequencing, and analysis

The mRNA libraries were prepared and sequenced at the GENEWIZ Bioinformatics Institute. Total RNA of each genotype was extracted from the mature leaves of 70-day-old wild-type and mutant plants using TRIzol reagent (Invitrogen). The total RNA of each sample was quantified and qualified by an Agilent 2100 Bioanalyzer (Agilent Technologies, Palo Alto, CA, USA) and NanoDrop spectrophotometer (Thermo Fisher Scientific Inc.). One microgram of total RNA with a RIN above 7 was used to purify poly (A) mRNA, and this mRNA was used for the synthesis and amplification of complementary DNA. The mRNA-seq libraries were prepared using the VAHTSTM mRNA-seq V2 Library Prep Kit for Illumina (Vazyme). Then, the libraries were sequenced on the Illumina HiSeq X Ten platform. For each library, > 6 Gb of raw data was generated (Supplemental Data Set S1). Adapters were removed from reads using Cutadapt (Martin, 2011) v1.18, and the reads were then mapped to the MSU7.0 reference genome using HISAT2 (Kim et al., 2015) v2.1.0 and quantified using StringTie (Pertea et al., 2016) v1.3.3b. Differentially expressed genes and TEs were identified in each mutant

with the criteria of a four-fold difference and an adjusted $P < 0.01$ (Stroud et al., 2013b) using HTSeq (Anders et al., 2015) v0.11.0 and DESeq2 (Love et al., 2014) v1.19.31.

Small RNA library construction, sequencing, and analysis

Small RNA libraries were prepared and sequenced at the GENEWIZ Bioinformatics Institute. In brief, small RNA-seq libraries were constructed from total RNAs extracted from the same tissues used for the mRNA libraries. RNA was purified as previously described (Thomas and Ansel, 2010) then followed by library construction with the NEXTflex Small RNA-Seq Kit (PerkinElmer). The libraries were sequenced on the same Illumina HiSeq X Ten platform as the mRNA-seq libraries. For each library, > 4 Gb of raw data was generated (Supplemental Data Set S1). Raw data were cleaned by removing adapters by Cutadapt (Martin, 2011) v1.18, and reads with lengths of 18-28 nt were retained. Then, the clean reads were uniquely mapped to the MSU7.0 reference genome using Bowtie (Langmead et al., 2009) v1.2.2, allowing no mismatches. The smRNA counts were normalized to the size of each library by dividing the number of reads by the number of unique reads with a length of 21 nt.

Chromatin-immunoprecipitation (ChIP) sequencing and analysis

We used public ChIP-seq data for the seedlings of rice (H3K9me1, GSM2084216 (Fang et al., 2016); H3K9me2, GSM2152477 (Tan et al., 2016); H3K9me3, GSM2084221 (Fang et al., 2016); H3K4me3, GSM2947265 (Zheng et al., 2019); H3K9ac, GSM2947268 (Zheng et al., 2019); H3K27ac, GSM2947267 (Zheng et al., 2019); H3K27me3, GSM2947270 (Zheng et al., 2019); H3K36me3, GSM2947266 (Zheng et al.,

2019); H4K12ac, GSM2947269 (Zheng et al., 2019)). Reads were mapped to MSU7.0 reference genome using Bowtie2 (Langmead and Salzberg, 2012) v2.3.4.3. The visualization program ngs.plot (Shen et al., 2014) (v2.47.1) is used on the sorted BAM file to create the average signal profiles.

Gene Ontology (GO) analysis

The R-Bioconductor package topGO v2.31.0 was used to perform the GO enrichment analysis involved in the biological processes (Alexa et al., 2006).

Accession numbers

The sequencing data generated in this study, including WGBS, mRNA-seq, and sRNA-seq data, have been deposited in GEO (GSE138705). The datasets of CHG-hypo and CHH-hypo DMRs analyzed in the study can be downloaded from Zenodo (https://doi.org/10.5281/zenodo.4851677) or GitHub repository (https://github.com/yimingfish/TPC_Supplemental-Data/tree/1.0).

SUPPLEMENTAL DATA

Supplemental Figure S1. Genotypic analysis of DNA methyltransferase mutations.

Supplemental Figure S2. CRISPR-Cas9-induced mutations in DNA methyltransferase genes.

Supplemental Figure S3. Effects of the non-CG methyltransferase mutations on plant growth.

Supplemental Figure S4. The different distribution proportions of different TE families in minor DNA methyltransferase mutant.

Supplemental Figure S5. OsDRM2, OsCMT2, and OsCMT3a cooperatively regulate CHH methylation.

Supplemental Figure S6. The relationship between non-CG methylation and transcriptome.

Supplemental Figure S7. The remaining mCHG and mCHH regions are completely overlapped with each other in *Os-dcc* mutants.

Supplemental Figure S8. The relationship between the mCHG/mCHH regions in *Os-dcc* mutant and GC content.

Supplemental Figure S9. Functional diversities of OsCMT3a and OsCMT3b.

Supplemental Figure S10. Phylogenetic relationships of CMTs across angiosperm.

Supplemental Figure S11. DNA methylation of *Os-dcc* hypo DMRs in CMT and RdDM mutants.

Supplemental Figure S12. The features of *Osdrm3* CHH DMRs.

Supplemental Figure S13. Characteristics of the non-CG DMRs between *Os-dcc* and *Os-ddccc* mutant.

Supplemental Table S1. Description of sgRNA target sites and sequences.

Supplemental Table S2. CRISPR-Cas9 vectors for DNA methyltransferase mutants.

Supplemental Table S3. The Gene Ontology (GO) analysis of genes overlapped with mCHG regions.

Supplemental Table S4. The Gene Ontology (GO) analysis of genes overlapped with mCHH regions.

Supplemental Table S5. PCR primers used in this study.

Supplemental Data Set S1. Summary of BS-seq, mRNA-seq and sRNA-seq libraries.

Supplemental Data Set S2. List of CHG-hypo DMRs and CHH-hypo DMRs between *Os-dcc* and *Os-ddccc* mutant.

Supplemental Data Set S3. List of differentially expressed genes (DEGs)/TEs in the mutants.

Supplemental File 1. Alignment corresponding to the phylogenetic tree in Supplemental Figure 10.

ACKNOWLEDGMENTS:

We are grateful for the useful comments and edits suggested by the anonymous reviewers. We thank all members of the Wang group and Zhai group for helpful discussion.

FUNDING:

The group of J.Z. is supported by the National Key R&D Program of China Grant (2019YFA0903903), an NSFC to J.Z. (31871234), the Program for Guangdong Introducing Innovative and Entrepreneurial Teams (2016ZT06S172), and the Shenzhen Sci-Tech Fund (KYTDPT20181011104005), and the Key Laboratory of Molecular Design for Plant Cell Factory of Guangdong Higher Education Institutes

(2019KSYS006). The group of K.W. is supported by the National Transgenic Science and Technology Program (2019ZX08010-003), the National Key Research and Development Program of China (2017YFD0102002), and the Agricultural Science and Technology Innovation Program of Chinese Academy of Agricultural Sciences. Work in the laboratory of X.Z. is supported by NSF (MCB-1552455).

AUTHOR CONTRIBUTIONS:

D.H., C.W., Y.L., D.L., B.L., and Y.L. performed the experiments. L.G., J.D., R.X., and X.Z. provided materials and data. Y.Y., C.W., J.J., and D.H. analyzed the data. J.Z. and K.W. oversaw the study. D.H., Y.Y., and J.Z. wrote the manuscript, and all authors revised the manuscript.

Data and materials availability: All data needed to evaluate the conclusions in the paper are present in the paper and/or the Supplementary Materials. Additional data related to this paper may be requested from the authors.

REFERENCES

Akalin, A., Kormaksson, M., Li, S., Garrett-Bakelman, F.E., Figueroa, M.E., Melnick, A., and Mason, C.E. (2012). methylKit: a comprehensive R package for the analysis of genome-wide DNA methylation profiles. Genome Biol. **13,** R87.

Alexa, A., Rahnenfuhrer, J., and Lengauer, T. (2006). Improved scoring of functional groups from gene expression data by decorrelating GO graph structure. Bioinformatics (Oxford, England) **22,** 1600-1607.

Anders, S., Pyl, P.T., and Huber, W. (2015). HTSeq—a Python framework to work with high-throughput sequencing data. Bioinformatics (Oxford, England) **31,** 166-169.

Bestor, T.H., and Verdine, G.L. (1994). DNA methyltransferases. Current opinion in cell biology **6,** 380-389.

Bewick, A.J., Niederhuth, C.E., Ji, L., Rohr, N.A., Griffin, P.T., Leebens-Mack, J., and Schmitz, R.J. (2017). The evolution of CHROMOMETHYLASES and gene body DNA methylation in plants. Genome biology **18,** 65.

Borges, F., and Martienssen, R.A. (2015). The expanding world of small RNAs in plants. Nat. Rev. Mol. Cell Biol. **16,** 727-741.

Cao, X., and Jacobsen, S.E. (2002). Locus-specific control of asymmetric and CpNpG methylation by the DRM and CMT3 methyltransferase genes. Proc Natl Acad Sci U S A **99 Suppl 4,** 16491-16498.

Cao, X., Aufsatz, W., Zilberman, D., Mette, M.F., Huang, M.S., Matzke, M., and Jacobsen, S.E. (2003). Role of the DRM and CMT3 methyltransferases in RNA-directed DNA methylation. Curr. Biol. **13,** 2212-2217.

Chen, K., Wang, Y., Zhang, R., Zhang, H., and Gao, C. (2019). CRISPR/Cas genome editing and precision plant breeding in agriculture. Annu. Rev. Plant Biol. **70,** 667-697.

Cheng, C., Tarutani, Y., Miyao, A., Ito, T., Yamazaki, M., Sakai, H., Fukai, E., and Hirochika, H. (2015). Loss of function mutations in the rice chromomethylase OsCMT3a cause a burst of transposition. Plant J. **83,** 1069-1081.

Du, J., Johnson, L.M., Jacobsen, S.E., and Patel, D.J. (2015). DNA methylation pathways and their crosstalk with histone methylation. Nat. Rev. Mol. Cell Biol. **16,** 519-532.

Du, J., Zhong, X., Bernatavichute, Y.V., Stroud, H., Feng, S., Caro, E., Vashisht, A.A., Terragni, J., Chin, H.G., Tu, A., Hetzel, J., Wohlschlegel, J.A., Pradhan, S., Patel, D.J., and Jacobsen, S.E. (2012). Dual binding of chromomethylase domains to H3K9me2-containing nucleosomes directs DNA methylation in plants. Cell **151,** 167-180.

Eichten, S.R., Briskine, R., Song, J., Li, Q., Swanson-Wagner, R., Hermanson, P.J., Waters, A.J., Starr, E., West, P.T., Tiffin, P., Myers, C.L., Vaughn, M.W., and Springer, N.M. (2013). Epigenetic and genetic influences on DNA methylation variation in maize populations. The Plant cell **25,** 2783-2797.

Fang, Y., Wang, X., Wang, L., Pan, X., Xiao, J., Wang, X.E., Wu, Y., and Zhang, W. (2016). Functional characterization of open chromatin in bidirectional promoters of rice. Sci Rep **6,** 32088.

Gouil, Q., and Baulcombe, D.C. (2016). DNA Methylation Signatures of the Plant Chromomethyltransferases. Plos Genet **12,** e1006526.

He, X.J., Chen, T., and Zhu, J.K. (2011). Regulation and function of DNA methylation in plants and animals. Cell Res. **21,** 442-465.

He, Y., and Ecker, J.R. (2015). Non-CG Methylation in the Human Genome. Annu Rev Genomics Hum Genet **16,** 55-77.

Henderson, I.R., Deleris, A., Wong, W., Zhong, X., Chin, H.G., Horwitz, G.A., Kelly, K.A., Pradhan, S., and Jacobsen, S.E. (2010). The de novo cytosine methyltransferase DRM2 requires intact UBA domains and a catalytically mutated paralog DRM3 during RNA-directed DNA methylation in Arabidopsis thaliana. Plos Genet **6,** e1001182.

Hu, L., Li, N., Xu, C., Zhong, S., Lin, X., Yang, J., Zhou, T., Yuliang, A., Wu, Y., Chen, Y.R., Cao, X., Zemach, A., Rustgi, S., von Wettstein, D., and Liu, B. (2014). Mutation of a major CG methylase in rice causes genome-wide

hypomethylation, dysregulated genome expression, and seedling lethality. Proc. Natl. Acad. Sci. USA **111,** 10642-10647.

Hu, X., Meng, X., Liu, Q., Li, J., and Wang, K. (2018). Increasing the efficiency of CRISPR-Cas9-VQR precise genome editing in rice. Plant Biotechnol. J. **16,** 292-297.

Huala, E., Dickerman, A.W., Garcia-Hernandez, M., Weems, D., Reiser, L., LaFond, F., Hanley, D., Kiphart, D., Zhuang, M., Huang, W., Mueller, L.A., Bhattacharyya, D., Bhaya, D., Sobral, B.W., Beavis, W., Meinke, D.W., Town, C.D., Somerville, C., and Rhee, S.Y. (2001). The Arabidopsis Information Resource (TAIR): a comprehensive database and web-based information retrieval, analysis, and visualization system for a model plant. Nucleic Acids Res. **29,** 102-105.

Jiao, Y., Peluso, P., Shi, J., Liang, T., Stitzer, M.C., Wang, B., Campbell, M.S., Stein, J.C., Wei, X., Chin, C.S., Guill, K., Regulski, M., Kumari, S., Olson, A., Gent, J., Schneider, K.L., Wolfgruber, T.K., May, M.R., Springer, N.M., Antoniou, E., McCombie, W.R., Presting, G.G., McMullen, M., Ross-Ibarra, J., Dawe, R.K., Hastie, A., Rank, D.R., and Ware, D. (2017). Improved maize reference genome with single-molecule technologies. Nature **546,** 524-527.

Jullien, P.E., Susaki, D., Yelagandula, R., Higashiyama, T., and Berger, F. (2012). DNA methylation dynamics during sexual reproduction in Arabidopsis thaliana. Curr. Biol. **22,** 1825-1830.

Kawahara, Y., de la Bastide, M., Hamilton, J.P., Kanamori, H., McCombie, W.R., Ouyang, S., Schwartz, D.C., Tanaka, T., Wu, J., Zhou, S., Childs, K.L., Davidson, R.M., Lin, H., Quesada-Ocampo, L., Vaillancourt, B., Sakai, H., Lee, S.S., Kim, J., Numa, H., Itoh, T., Buell, C.R., and Matsumoto, T. (2013). Improvement of the Oryza sativa Nipponbare reference genome using next generation sequence and optical map data. Rice **6,** 4.

Kim, D., Langmead, B., and Salzberg, S.L. (2015). HISAT: a fast spliced aligner with low memory requirements. Nat. Methods **12,** 357-360.

Knott, G.J., and Doudna, J.A. (2018). CRISPR-Cas guides the future of genetic engineering. Science **361,** 866-869.

Lang, Z., Lei, M., Wang, X., Tang, K., Miki, D., Zhang, H., Mangrauthia, S.K., Liu, W., Nie, W., Ma, G., Yan, J., Duan, C.G., Hsu, C.C., Wang, C., Tao, W.A., Gong, Z., and Zhu, J.K. (2015). The methyl-CpG-binding protein MBD7 facilitates active DNA demethylation to limit DNA hyper-methylation and transcriptional gene silencing. Mol Cell **57,** 971-983.

Langmead, B., and Salzberg, S.L. (2012). Fast gapped-read alignment with Bowtie 2. Nature methods **9,** 357-359.

Langmead, B., Trapnell, C., Pop, M., and Salzberg, S.L. (2009). Ultrafast and memory-efficient alignment of short DNA sequences to the human genome. Genome Biol. **10,** R25.

Law, J.A., and Jacobsen, S.E. (2010). Establishing, maintaining and modifying DNA methylation patterns in plants and animals. Nature Rev. Genet. **11,** 204-220.

Li, D., Palanca, A.M.S., Won, S.Y., Gao, L., Feng, Y., Vashisht, A.A., Liu, L., Zhao, Y., Liu, X., Wu, X., Li, S., Le, B., Kim, Y.J., Yang, G., Li, S., Liu, J., Wohlschlegel, J.A., Guo, H., Mo, B., Chen, X., and Law, J.A. (2017a). The

MBD7 complex promotes expression of methylated transgenes without significantly altering their methylation status. Elife **6**.

Li, J., Sun, Y., Du, J., Zhao, Y., and Xia, L. (2017b). Generation of targeted point mutations in rice by a modified CRISPR/Cas9 system. Mol. Plant **10,** 526-529.

Li, Q., Gent, J.I., Zynda, G., Song, J., Makarevitch, I., Hirsch, C.D., Hirsch, C.N., Dawe, R.K., Madzima, T.F., McGinnis, K.M., Lisch, D., Schmitz, R.J., Vaughn, M.W., and Springer, N.M. (2015). RNA-directed DNA methylation enforces boundaries between heterochromatin and euchromatin in the maize genome. Proc Natl Acad Sci U S A **112,** 14728-14733.

Li, Q., Eichten, S.R., Hermanson, P.J., Zaunbrecher, V.M., Song, J., Wendt, J., Rosenbaum, H., Madzima, T.F., Sloan, A.E., Huang, J., Burgess, D.L., Richmond, T.A., McGinnis, K.M., Meeley, R.B., Danilevskaya, O.N., Vaughn, M.W., Kaeppler, S.M., Jeddeloh, J.A., and Springer, N.M. (2014). Genetic perturbation of the maize methylome. The Plant cell **26,** 4602-4616.

Lin, J.Y., Le, B.H., Chen, M., Henry, K.F., Hur, J., Hsieh, T.F., Chen, P.Y., Pelletier, J.M., Pellegrini, M., Fischer, R.L., Harada, J.J., and Goldberg, R.B. (2017). Similarity between soybean and Arabidopsis seed methylomes and loss of non-CG methylation does not affect seed development. Proc. Natl. Acad. Sci. USA **114,** E9730-e9739.

Lister, R., O'Malley, R.C., Tonti-Filippini, J., Gregory, B.D., Berry, C.C., Millar, A.H., and Ecker, J.R. (2008). Highly integrated single-base resolution maps of the epigenome in Arabidopsis. Cell **133,** 523-536.

Lister, R., Pelizzola, M., Dowen, R.H., Hawkins, R.D., Hon, G., Tonti-Filippini, J., Nery, J.R., Lee, L., Ye, Z., Ngo, Q.M., Edsall, L., Antosiewicz-Bourget, J., Stewart, R., Ruotti, V., Millar, A.H., Thomson, J.A., Ren, B., and Ecker, J.R. (2009). Human DNA methylomes at base resolution show widespread epigenomic differences. Nature **462,** 315-322.

Liu, Q., Wang, C., Jiao, X., Zhang, H., Song, L., Li, Y., Gao, C., and Wang, K. (2019). Hi-TOM: a platform for high-throughput tracking of mutations induced by CRISPR/Cas systems. Sci. China C Life Sci. **62,** 1-7.

Long, J., Liu, J., Xia, A., Springer, N.M., and He, Y. (2021). Maize Decrease in DNA methylation 1 targets RNA-directed DNA methylation on active chromatin. The Plant cell.

Love, M.I., Huber, W., and Anders, S. (2014). Moderated estimation of fold change and dispersion for RNA-seq data with DESeq2. Genome Biol. **15,** 550.

Martin, M. (2011). Cutadapt removes adapter sequences from high-throughput sequencing reads. EMBnet.journal **17,** 10-12.

Matzke, M.A., and Mosher, R.A. (2014). RNA-directed DNA methylation: an epigenetic pathway of increasing complexity. Nature Rev. Genet. **15,** 394-408.

McCormick, R.F., Truong, S.K., Sreedasyam, A., Jenkins, J., Shu, S., Sims, D., Kennedy, M., Amirebrahimi, M., Weers, B.D., McKinley, B., Mattison, A., Morishige, D.T., Grimwood, J., Schmutz, J., and Mullet, J.E. (2018). The Sorghum bicolor reference genome: improved assembly, gene annotations, a transcriptome atlas, and signatures of genome organization. Plant J. **93,** 338-354.

Moritoh, S., Eun, C.H., Ono, A., Asao, H., Okano, Y., Yamaguchi, K., Shimatani, Z., Koizumi, A., and Terada, R. (2012). Targeted disruption of an orthologue of

DOMAINS REARRANGED METHYLASE 2, OsDRM2, impairs the growth of rice plants by abnormal DNA methylation. Plant J. **71,** 85-98.

Niederhuth, C.E., Bewick, A.J., Ji, L., Alabady, M.S., Kim, K.D., Li, Q., Rohr, N.A., Rambani, A., Burke, J.M., Udall, J.A., Egesi, C., Schmutz, J., Grimwood, J., Jackson, S.A., Springer, N.M., and Schmitz, R.J. (2016). Widespread natural variation of DNA methylation within angiosperms. Genome Biol. **17,** 194.

Pertea, M., Kim, D., Pertea, G.M., Leek, J.T., and Salzberg, S.L. (2016). Transcript-level expression analysis of RNA-seq experiments with HISAT, StringTie and Ballgown. Nat. Protoc. **11,** 1650-1667.

Ronemus, M.J., Galbiati, M., Ticknor, C., Chen, J., and Dellaporta, S.L. (1996). Demethylation-induced developmental pleiotropy in Arabidopsis. Science **273,** 654-657.

Schultz, M.D., Schmitz, R.J., and Ecker, J.R. (2012). 'Leveling' the playing field for analyses of single-base resolution DNA methylomes. Trends in genetics : TIG **28,** 583-585.

Schultz, M.D., He, Y., Whitaker, J.W., Hariharan, M., Mukamel, E.A., Leung, D., Rajagopal, N., Nery, J.R., Urich, M.A., Chen, H., Lin, S., Lin, Y., Jung, I., Schmitt, A.D., Selvaraj, S., Ren, B., Sejnowski, T.J., Wang, W., and Ecker, J.R. (2015). Human body epigenome maps reveal noncanonical DNA methylation variation. Nature **523,** 212-216.

Sharma, R., Mohan Singh, R.K., Malik, G., Deveshwar, P., Tyagi, A.K., Kapoor, S., and Kapoor, M. (2009). Rice cytosine DNA methyltransferases — gene expression profiling during reproductive development and abiotic stress. FEBS J. **276,** 6301-6311.

Shearer, L.A., Anderson, L.K., de Jong, H., Smit, S., Goicoechea, J.L., Roe, B.A., Hua, A., Giovannoni, J.J., and Stack, S.M. (2014). Fluorescence in situ hybridization and optical mapping to correct scaffold arrangement in the tomato genome. G3: Genes | Genomes | Genetics **4,** 1395-1405.

Shen, L., Shao, N., Liu, X., and Nestler, E. (2014). ngs.plot: Quick mining and visualization of next-generation sequencing data by integrating genomic databases. BMC genomics **15,** 284.

Smarda, P., Bures, P., Horova, L., Leitch, I.J., Mucina, L., Pacini, E., Tichy, L., Grulich, V., and Rotreklova, O. (2014). Ecological and evolutionary significance of genomic GC content diversity in monocots. Proc. Natl. Acad. Sci. USA **111,** E4096-4102.

Song, Q., Jenkins, J., Jia, G., Hyten, D.L., Pantalone, V., Jackson, S.A., Schmutz, J., and Cregan, P.B. (2016). Construction of high resolution genetic linkage maps to improve the soybean genome sequence assembly Glyma1.01. BMC genomics **17,** 33.

Song, X., Li, Y., Cao, X., and Qi, Y. (2019). MicroRNAs and their regulatory roles in plant-environment interactions. Annu. Rev. Plant Biol. **70,** 489-525.

Stroud, H., Greenberg, M.V., Feng, S., Bernatavichute, Y.V., and Jacobsen, S.E. (2013a). Comprehensive analysis of silencing mutants reveals complex regulation of the Arabidopsis methylome. Cell **152,** 352-364.

Stroud, H., Do, T., Du, J., Zhong, X., Feng, S., Johnson, L., Patel, D.J., and Jacobsen, S.E. (2014). Non-CG methylation patterns shape the epigenetic landscape in Arabidopsis. Nature Struct. Mol. Biol. **21,** 64-72.

Stroud, H., Ding, B., Simon, S.A., Feng, S., Bellizzi, M., Pellegrini, M., Wang, G.L., Meyers, B.C., and Jacobsen, S.E. (2013b). Plants regenerated from tissue culture contain stable epigenome changes in rice. eLife **2,** e00354.

Tan, F., Zhou, C., Zhou, Q., Zhou, S., Yang, W., Zhao, Y., Li, G., and Zhou, D.X. (2016). Analysis of chromatin regulators reveals specific features of rice DNA methylation pathways. Plant Physiol. **171,** 2041-2054.

Tatarinova, T.V., Alexandrov, N.N., Bouck, J.B., and Feldmann, K.A. (2010). GC3 biology in corn, rice, sorghum and other grasses. BMC genomics **11,** 308.

Thomas, M.F., and Ansel, K.M. (2010). Construction of small RNA cDNA libraries for deep sequencing. Methods in molecular biology (Clifton, N.J.) **667,** 93-111.

Turco, G.M., Kajala, K., Kunde-Ramamoorthy, G., Ngan, C.Y., Olson, A., Deshphande, S., Tolkunov, D., Waring, B., Stelpflug, S., Klein, P., Schmutz, J., Kaeppler, S., Ware, D., Wei, C.L., Etchells, J.P., and Brady, S.M. (2017). DNA methylation and gene expression regulation associated with vascularization in Sorghum bicolor. New Phytol. **214,** 1213-1229.

Vogel, J.P., Garvin, D.F., Mockler, T.C., Schmutz, J., Rokhsar, D., Bevan, M.W., Barry, K., Lucas, S., Harmon-Smith, M., Lail, K., Tice, H., Schmutz, J., Grimwood, J., McKenzie, N., Bevan, M.W., Huo, N., Gu, Y.Q., Lazo, G.R., Anderson, O.D., Vogel, J.P., You, F.M., Luo, M.-C., Dvorak, J., Wright, J., Febrer, M., Bevan, M.W., Idziak, D., Hasterok, R., Garvin, D.F., Lindquist, E., Wang, M., Fox, S.E., Priest, H.D., Filichkin, S.A., Givan, S.A., Bryant, D.W., Chang, J.H., Mockler, T.C., Wu, H., Wu, W., Hsia, A.-P., Schnable, P.S., Kalyanaraman, A., Barbazuk, B., Michael, T.P., Hazen, S.P., Bragg, J.N., Laudencia-Chingcuanco, D., Vogel, J.P., Garvin, D.F., Weng, Y., McKenzie, N., Bevan, M.W., Haberer, G., Spannagl, M., Mayer, K., Rattei, T., Mitros, T., Rokhsar, D., Lee, S.-J., Rose, J.K.C., Mueller, L.A., York, T.L., Wicker, T., Buchmann, J.P., Tanskanen, J., Schulman, A.H., Gundlach, H., Wright, J., Bevan, M., Costa de Oliveira, A., da C. Maia, L., Belknap, W., Gu, Y.Q., Jiang, N., Lai, J., Zhu, L., Ma, J., Sun, C., Pritham, E., Salse, J., Murat, F., Abrouk, M., Haberer, G., Spannagl, M., Mayer, K., Bruggmann, R., Messing, J., You, F.M., Luo, M.-C., Dvorak, J., Fahlgren, N., Fox, S.E., Sullivan, C.M., Mockler, T.C., Carrington, J.C., Chapman, E.J., May, G.D., Zhai, J., Ganssmann, M., Guna Ranjan Gurazada, S., German, M., Meyers, B.C., Green, P.J., Bragg, J.N., Tyler, L., Wu, J., Gu, Y.Q., Lazo, G.R., Laudencia-Chingcuanco, D., Thomson, J., Vogel, J.P., Hazen, S.P., Chen, S., Scheller, H.V., Harholt, J., Ulvskov, P., Fox, S.E., Filichkin, S.A., Fahlgren, N., Kimbrel, J.A., Chang, J.H., Sullivan, C.M., Chapman, E.J., Carrington, J.C., Mockler, T.C., Bartley, L.E., Cao, P., Jung, K.-H., Sharma, M.K., Vega-Sanchez, M., Ronald, P., Dardick, C.D., De Bodt, S., Verelst, W., Inzé, D., Heese, M., Schnittger, A., Yang, X., Kalluri, U.C., Tuskan, G.A., Hua, Z., Vierstra, R.D., Garvin, D.F., Cui, Y., Ouyang, S., Sun, Q., Liu, Z., Yilmaz, A., Grotewold, E., Sibout, R., Hematy, K., Mouille, G., Höfte, H., Michael, T., Pelloux, J., O'Connor, D., Schnable, J., Rowe, S., Harmon, F., Cass, C.L.,

Sedbrook, J.C., Byrne, M.E., Walsh, S., Higgins, J., Bevan, M., Li, P., Brutnell, T., Unver, T., Budak, H., Belcram, H., Charles, M., Chalhoub, B., Baxter, I., The International Brachypodium, I., Principal, i., sequencing, D.N.A., assembly, Pseudomolecule, a., sequencing, B.A.C.e., Transcriptome, s., analysis, Gene, a., annotation, Repeats, a., Comparative, g., Small, R.N.A.a., Manual, a., and gene family, a. (2010). Genome sequencing and analysis of the model grass Brachypodium distachyon. Nature **463,** 763-768.

Wang, C., Shen, L., Fu, Y., Yan, C., and Wang, K. (2015). A simple CRISPR/Cas9 system for multiplex genome editing in rice. J. Genet. Genom. **42,** 703-706.

Xi, Y., and Li, W. (2009). BSMAP: whole genome bisulfite sequence MAPping program. BMC bioinformatics **10,** 232.

Xie, W., Barr, C.L., Kim, A., Yue, F., Lee, A.Y., Eubanks, J., Dempster, E.L., and Ren, B. (2012). Base-resolution analyses of sequence and parent-of-origin dependent DNA methylation in the mouse genome. Cell **148,** 816-831.

Yamauchi, T., Johzuka-Hisatomi, Y., Terada, R., Nakamura, I., and Iida, S. (2014). The MET1b gene encoding a maintenance DNA methyltransferase is indispensable for normal development in rice. Plant Mol. Biol. **85,** 219-232.

Yamauchi, T., Johzuka-Hisatomi, Y., Fukada-Tanaka, S., Terada, R., Nakamura, I., and Iida, S. (2009). Homologous recombination-mediated knock-in targeting of the MET1a gene for a maintenance DNA methyltransferase reproducibly reveals dosage-dependent spatiotemporal gene expression in rice. Plant J. **60,** 386-396.

Yu, J., Hu, S., Wang, J., Wong, G.K.-S., Li, S., Liu, B., Deng, Y., Dai, L., Zhou, Y., Zhang, X., Cao, M., Liu, J., Sun, J., Tang, J., Chen, Y., Huang, X., Lin, W., Ye, C., Tong, W., Cong, L., Geng, J., Han, Y., Li, L., Li, W., Hu, G., Huang, X., Li, W., Li, J., Liu, Z., Li, L., Liu, J., Qi, Q., Liu, J., Li, L., Li, T., Wang, X., Lu, H., Wu, T., Zhu, M., Ni, P., Han, H., Dong, W., Ren, X., Feng, X., Cui, P., Li, X., Wang, H., Xu, X., Zhai, W., Xu, Z., Zhang, J., He, S., Zhang, J., Xu, J., Zhang, K., Zheng, X., Dong, J., Zeng, W., Tao, L., Ye, J., Tan, J., Ren, X., Chen, X., He, J., Liu, D., Tian, W., Tian, C., Xia, H., Bao, Q., Li, G., Gao, H., Cao, T., Wang, J., Zhao, W., Li, P., Chen, W., Wang, X., Zhang, Y., Hu, J., Wang, J., Liu, S., Yang, J., Zhang, G., Xiong, Y., Li, Z., Mao, L., Zhou, C., Zhu, Z., Chen, R., Hao, B., Zheng, W., Chen, S., Guo, W., Li, G., Liu, S., Tao, M., Wang, J., Zhu, L., Yuan, L., and Yang, H. (2002). A Draft Sequence of the Rice Genome (Oryza sativa L. ssp. indica). Science **296,** 79-92.

Zemach, A., Kim, M.Y., Hsieh, P.H., Coleman-Derr, D., Eshed-Williams, L., Thao, K., Harmer, S.L., and Zilberman, D. (2013). The Arabidopsis nucleosome remodeler DDM1 allows DNA methyltransferases to access H1-containing heterochromatin. Cell **153,** 193-205.

Zhang, H., Lang, Z., and Zhu, J.K. (2018). Dynamics and function of DNA methylation in plants. Nat. Rev. Mol. Cell Biol. **19,** 489-506.

Zheng, D., Wang, L., Chen, L., Pan, X., Lin, K., Fang, Y., Wang, X.E., and Zhang, W. (2019). Salt-Responsive Genes are Differentially Regulated at the Chromatin Levels Between Seedlings and Roots in Rice. Plant Cell Physiol **60,** 1790-1803.

Zhong, X., Hale, C.J., Nguyen, M., Ausin, I., Groth, M., Hetzel, J., Vashisht, A.A., Henderson, I.R., Wohlschlegel, J.A., and Jacobsen, S.E. (2015). Domains

rearranged methyltransferase3 controls DNA methylation and regulates RNA polymerase V transcript abundance in Arabidopsis. Proc Natl Acad Sci U S A **112,** 911-916.

Zhou, M., Palanca, A.M.S., and Law, J.A. (2018). Locus-specific control of the de novo DNA methylation pathway in Arabidopsis by the CLASSY family. Nature genetics **50,** 865-873.

Figure Legends

Figure 1. CRISPR-Cas9 knockout of DNA methyltransferase genes and phenotypes of T1 mutants.

(A) Schematic illustrations of non-CG methyltransferase gene regions targeted by the guide RNA. Dark blue lines indicate introns, light blue bars indicate exons, and white bars indicate UTRs (untranslated regions). The guide RNA target sequences are colored in red. **(B)** Genotypic analysis of T1 plants, 8 single-KO mutants and 8 multiple-KO mutants obtained and used for NGS. In the table, "I" stands for insertion, "D" stands for deletion, and the number before "I" or "D" stands for the number of base pair insertion or deletion.**(C)** Phenotypic analysis of selected single and multiple knockout mutants from T1 progeny (See Supplemental Figure 3 for additional mutants). DAG: Days After Germination. Scale bars = 5 cm.

Figure 2. Functional identification of non-CG methyltransferases involved in DNA methylation.

(A) Heatmap of rice mCHG regions. The columns represent the indicated genotypes, and the rows represent the mCHG sites. The rows were sorted by complete linkage hierarchical clustering with Euclidean distance as the distance measure. Rows with grey color indicated the sites with insufficient coverage. **(B)** Heatmap of rice mCHH regions. The heatmap shows the methylation status of all 200 bp bins that have passed the DMR filter. All bins are of equal size, and we merged adjacent bins for clustering DMRs to organize rows in the heatmap figures. **(C** to **E)** Genome browser views of CHG methylation of rice chromosomes in *Oscmt3a* CHG DMRs **(C)**, *Osdrm2* CHG DMRs **(D)**, and *Osdrm2*/*cmt3a* CHG DMRs **(E)**. Genes (blue bars) and TEs (yellow bars) are shown below. **(F** to **I)** Genome browser views of CHH methylation of rice chromosomes in *Osdrm2* CHH DMRs **(F)** *Oscmt2* CHH DMRs **(G)** *Oscmt3a* CHH DMRs **(H)** and *Oscmt2*/*cmt3a* CHH DMRs **(I)**. **(J)** Number of TEs defined as having differential expression in the indicated genotypes. **(K)** Boxplots of TE expression change in *Os-dcc* mutants relative to the wild type in the indicated genotypes. Boxes with different letters indicate significant differences at $P < 0.01$ level based on the two-tailed Wilcoxon rank-sum test. **(L)** 24-nt siRNA levels in *Os-dcc* mutant non-CG DMRs. 24-nt siRNA levels

were normalized by 21-nt siRNA levels for each genotype. Asterisks indicate significant differences compared with control based on the two-tailed Wilcoxon rank-sum test (*P < 0.01).

Figure 3. The mCHG and mCHH regions in rice *Os-dcc* mutants feature a high GC content.

(A) Percentage of the mCHG and mCHH regions in rice *Os-dcc*/*ddccc* mutants and Arabidopsis *ddcc* mutants. **(B)** Genome browser views of CG, CHG, and CHH methylation of rice chromosomes in the mCHG and mCHH regions in *Os-dcc*. TEs (yellow bars) are shown below. **(C** and **D)** Average cytosine methylation levels in the CHG context of mCHG regions **(C)** and CHH context of mCHH regions **(D)** plotted against the GC content (CG, CHG, and CHH contexts) for control, *Osdrm2*, *Oscmt2*, *Oscmt3a*, *Os-dcc* mutant and *Os-ddccc* mutant (from left to right). The data point density plots were calculated using 200bp fixed bins across the genome. The data point density bar indicates the values of two-dimensional kernel density estimation. (**E** and **F)** Average cytosine methylation levels in the CHG context of mCHG regions **(E)** and CHH context of mCHH regions **(F)** plotted against GC content for Arabidopsis: WT and *ddcc* mutants. The data point density bar indicates the values of two-dimensional kernel density estimation. N: the number of mCHG/mCHH regions. The dashed line **(C** to **F)** locates at 0.5 of GC content and divides the highly GC-rich regions with GC content 0.5~1. Note: to define methylated CHG (mCHG) and methylated CHH (mCHH) sites, the control library for 200bp bins was filtered first to ensure that methylation level no less than 0.5 for CHG context, and no less than 0.1 for CHH context.

Figure 4. Characteristics of the non-CG methylation regions in *Os-dcc* mutant with high GC content.

(A) Expression level of genes in mCHG/mCHH sites in *Os-dcc* and whole genome. **(B)** Expression level of TEs in mCHG/mCHH sites in *Os-dcc* and whole genome. **(C)** 24-nt siRNA levels in mCHG/mCHH sites in *Os-dcc* and whole genome. 24-nt siRNA levels were normalized by 21-nt siRNA levels for each kind of site. Asterisks indicate statistically significant differences compared with the expression level of genes (**A**), TEs

(**B**), and siRNA abundance (**C**) in whole genome (two-tailed Wilcoxon rank-sum test: *P < 0.01). **(D)** The different distribution proportions of different TE families between the mCHG/mCHH sites in *Os-dcc* and whole genome. **(E)** The percentage of genomic contents between mCHG/mCHH sites in *Os-dcc* and whole genome. **(F)** The different distribution of H3K9 markers the non-CG methylation sites in *Os-dcc*, TEs, and genes. **(G)** The different distribution of other histone modifications between the non-CG methylation sites in *Os-dcc*, TEs, and genes.

Figure 5. The GC-rich cluster of mCHG and mCHH sites are distinct in rice and catalyzed by OsCMT3b.

(A) Average cytosine methylation levels in the CHG context of mCHG regions plotted against GC content for *Brachypodium distachyon*, *Zea mays*, *Sorghum bicolor*, *Glycine max*, and *Solanum lycopersicum*. B73 and Mo17 are different maize cultivars. **(B)** Average cytosine methylation levels in the CHH context of mCHH regions plotted against GC content for *Brachypodium distachyon*, *Zea mays*, *Sorghum bicolor*, *Glycine max*, and *Solanum lycopersicum*. The data point density plots were calculated using 200bp fixed bins across the genome. (**C**) Average cytosine methylation levels in the CHG context of CHG-DMRs between *Os-dcc* and *Os-ddccc* in *Os-dcc*, *Os-ddcc* and *Os-ddccc* mutants. (**D**) Average cytosine methylation levels in the CHH context of CHH-DMRs between *Os-dcc* and *Os-ddccc* in *Os-dcc*, *Os-ddcc* and *Os-ddccc* mutants. The data point density bar indicates the values of two-dimensional kernel density estimation. N: the number of mCHG/mCHH regions. The dashed line **(A - D)** locates at 0.5 of GC content and divides the highly GC-rich regions with GC content 0.5~1.

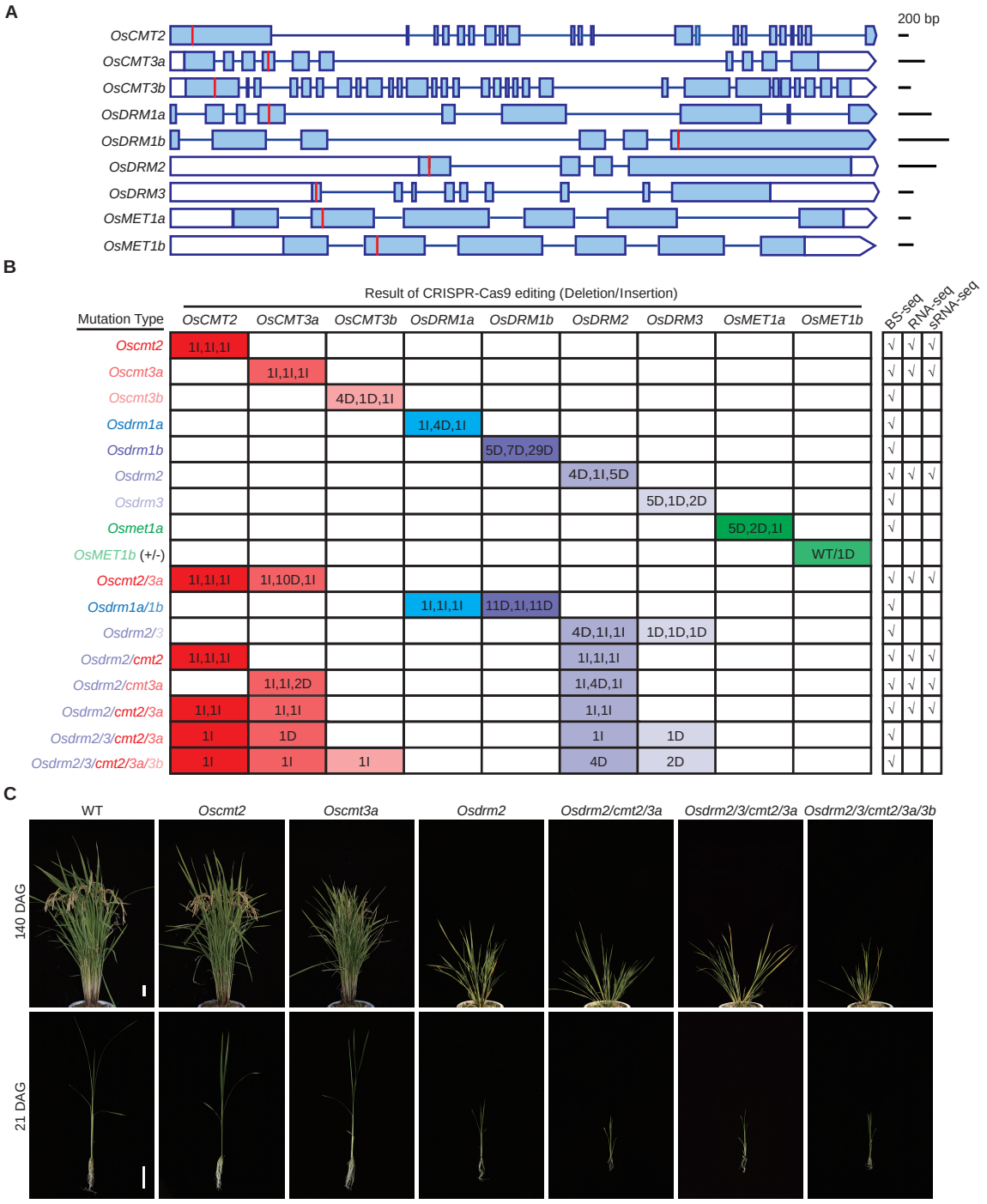

Figure 1. CRISPR-Cas9 knockout of DNA methyltransferase genes and phenotypes of T1 mutants.
(**A**) Schematic illustrations of non-CG methyltransferase gene regions targeted by the guide RNA. Dark blue lines indicate introns, light blue bars indicate exons, and white bars indicate UTRs (untranslated regions). The guide RNA target sequences are colored in red. (**B**) Genotypic analysis of T1 plants, 8 single-KO mutants and 8 multiple-KO mutants obtained and used for NGS. (**C**) Phenotypic analysis of selected single and multiple knockout mutants from T1 progeny (See fig. S3 for additional mutants). In the table, "I" stands for insertion, "D" stands for deletion, and the number before "I" or "D" stands for the number of base pair insertion or deletion. DAG: Day After Germination. Scale bars = 5 cm.

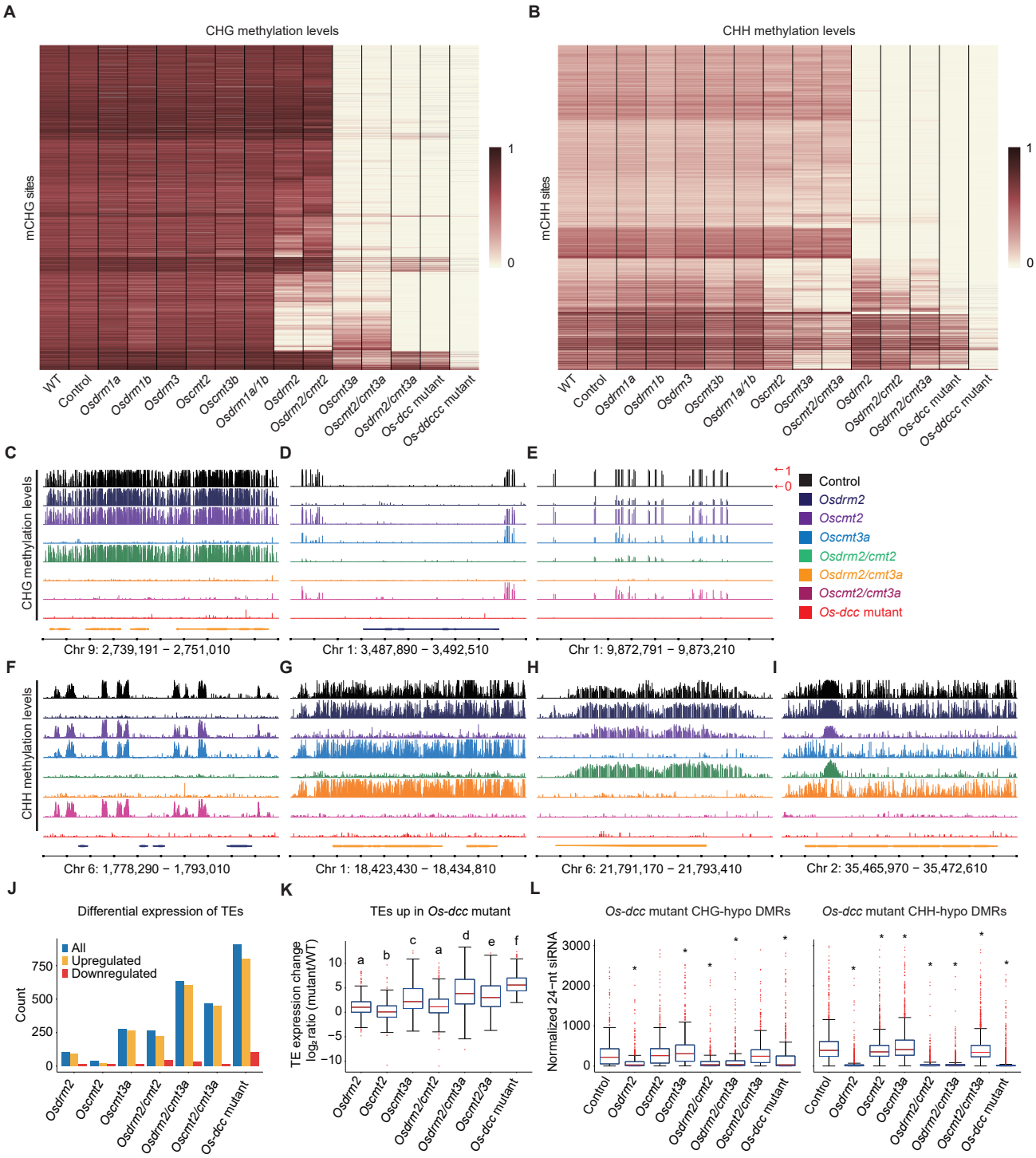

Figure 2. Functional identification of non-CG methyltransferases involved in DNA methylation.

(**A**) Heatmap of rice mCHG regions. The columns represent the indicated genotypes, and the rows represent the mCHG sites. The rows were sorted by complete linkage hierarchical clustering with Euclidean distance as the distance measure. Rows with grey color indicated the sites with insufficient coverage. (**B**) Heatmap of rice mCHH regions. The heatmap shows the methylation status of all 200 bp bins that have passed the DMR filter. All bins are of equal size, and we merged adjacent bins for clustering DMRs to organize rows in the heatmap figures. (**C** to **E**) Genome browser views of CHG methylation of rice chromosomes in *Oscmt3a* CHG DMRs (C), *Osdrm2* CHG DMRs (D), and *Osdrm2*/*cmt3a* CHG DMRs (**E**). Genes (blue bars) and TEs (yellow bars) are shown below. (**F** to **I**) Genome browser views of CHH methylation of rice chromosomes in *Osdrm2* CHH DMRs (**F**) *Oscmt2* CHH DMRs (**G**) *Oscmt3a* CHH DMRs (**H**) and *Oscmt2/cmt3a* CHH DMRs (**I**). (**J**) Number of TEs defined as having differential expression in the indicated genotypes. (**K**) Boxplots of TE expression change in *Os-dcc* mutants relative to the wild type in the indicated genotypes. Boxes with different letters indicate significant differences at $P < 0.01$ level based on the two-tailed Wilcoxon rank-sum test. (**L**) 24-nt siRNA levels in *Os-dcc* mutant non-CG DMRs. 24-nt siRNA levels were normalized by 21-nt siRNA levels for each genotype. Asterisks indicate significant differences compared with control based on the two-tailed Wilcoxon rank-sum test (*$P < 0.01$).

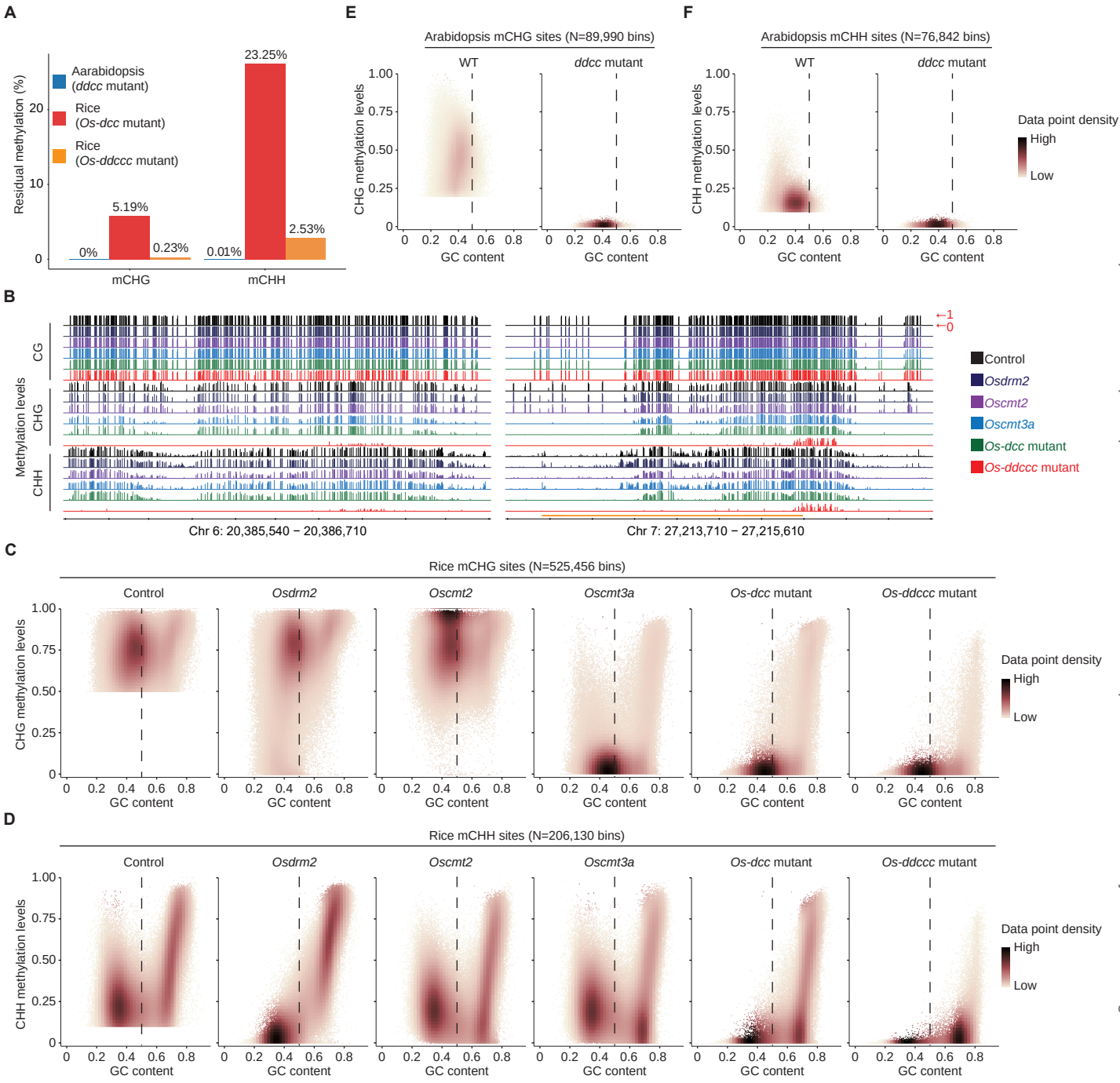

Figure 3. The mCHG and mCHH regions in rice *Os-dcc* mutants feature a high GC content.

(**A**) Percentage of the mCHG and mCHH regions in rice *Os-dcc*/*ddccc* mutants and Arabidopsis *ddcc* mutants. (**B**) Genome browser views of CG, CHG, and CHH methylation of rice chromosomes in the mCHG and mCHH regions in *Os-dcc*. TEs (yellow bars) are shown below. (**C** and **D**) Average cytosine methylation levels in the CHG context of mCHG regions (**C**) and CHH context of mCHH regions (**D**) plotted against the GC content (CG, CHG, and CHH contexts) for control, *Osdrm2*, *Oscmt2*, *Oscmt3a*, *Os-dcc* mutant and *Os-ddccc* mutant (from left to right). The data point density plots were calculated using 200bp fixed bins across the genome. The data point density bar indicates the values of two-dimensional kernel density estimation. (**E** and **F**) Average cytosine methylation levels in the CHG context of mCHG regions (**E**) and CHH context of mCHH regions (**F**) plotted against GC content for Arabidopsis: WT and *ddcc* mutants. The data point density bar indicates the values of two-dimensional kernel density estimation. N: the number of mCHG/mCHH regions. The dashed line (**C** to **F**) locates at 0.5 of GC content, and divides the highly GC-rich regions with GC content 0.5~1. Note: to define methylated CHG (mCHG) and methylated CHH (mCHH) sites, control library for 200bp bins was filtered first to ensure that methylation level no less than 0.5 for CHG context, and no less than 0.1 for CHH context.

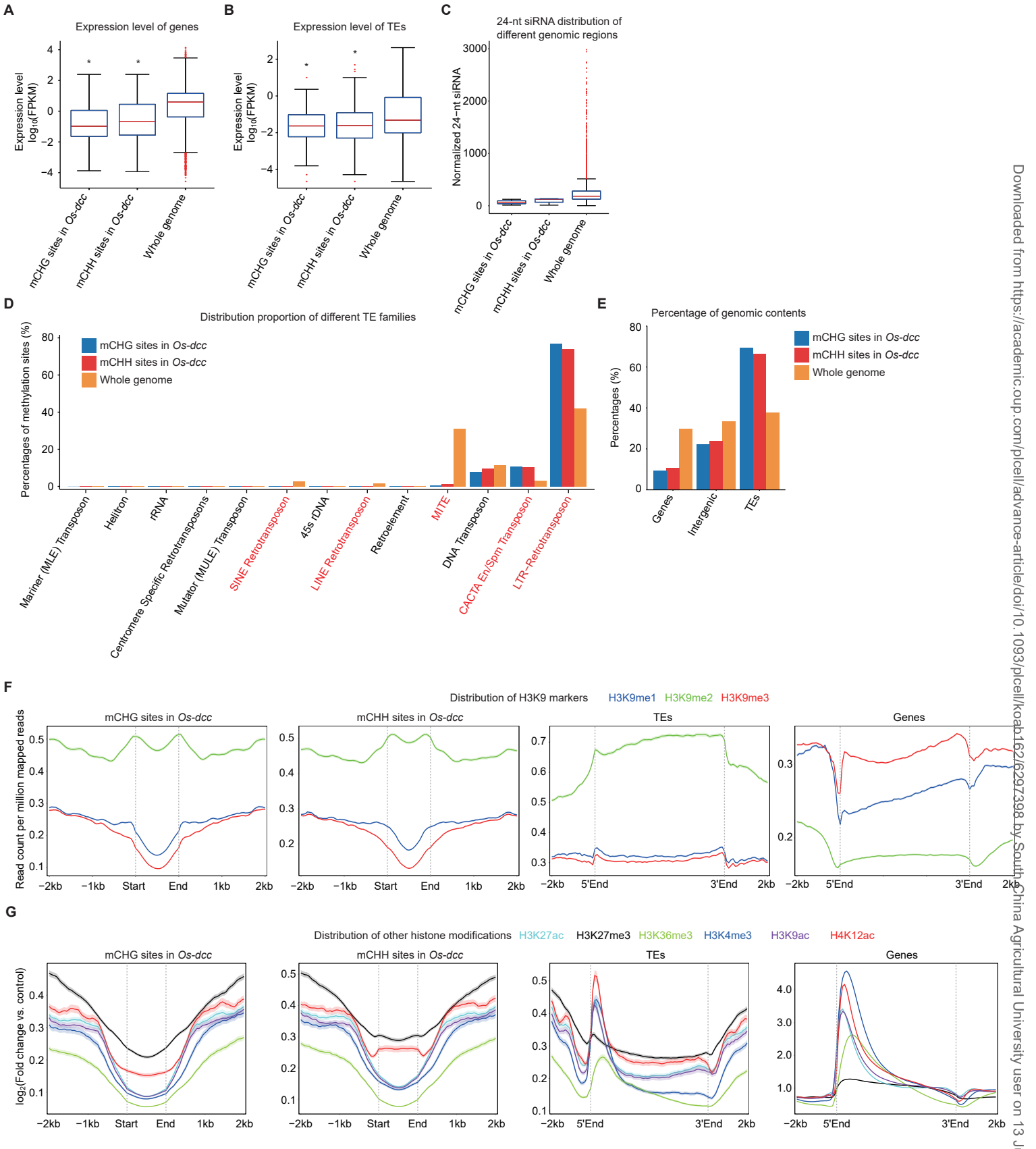

Figure 4. Characteristics of the non-CG methylation regions in *Os-dcc* mutant with high GC content.

(**A**) Expression level of genes in mCHG/mCHH sites in *Os-dcc* and whole genome. (**B**) Expression level of TEs in mCHG/mCHH sites in *Os-dcc* and whole genome. (**C**) 24-nt siRNA levels in mCHG/mCHH sites in *Os-dcc* and whole genome. 24-nt siRNA levels were normalized by 21-nt siRNA levels for each kind site. Asterisks indicate statistically significant differences compared with the expression level of gene (**A**), TEs (**B**), and siRNA abundance (**C**) in whole genome (two-tailed Wilcoxon rank-sum test: $*P < 0.01$). (**D**) The different distribution proportion of different TE families between the mCHG/mCHH sites in *Os-dcc* and whole genome. (**E**) The percentage of genomic contents between mCHG/mCHH sites in *Os-dcc* and whole genome. (**F**) The different distribution of H3K9 markers the non-CG methylation sites in *Os-dcc*, TEs, and genes. (**G**) The different distribution of other histon modifications between the non-CG methylation sites in *Os-dcc*, TEs, and genes.

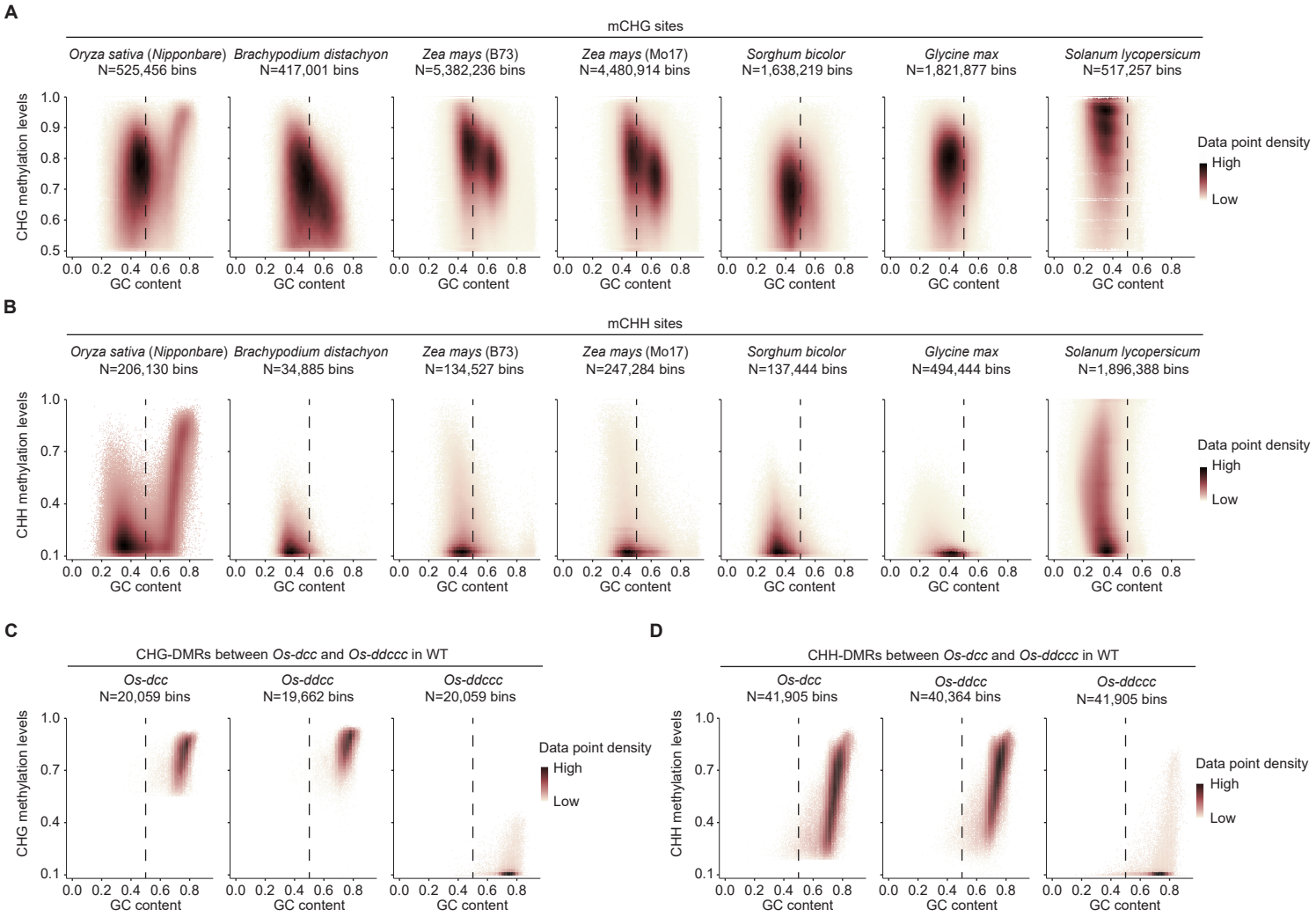

Figure 5. The GC-rich cluster of mCHG and mCHH sites are distinct in rice and catalyzed by OsCMT3b.

(**A**) Average cytosine methylation levels in the CHG context of mCHG regions plotted against GC content for *Brachypodium distachyon*, *Zea mays*, *Sorghum bicolor*, *Glycine max*, and *Solanum lycopersicum*. B73 and Mo17 are different maize cultivars. (**B**) Average cytosine methylation levels in the CHH context of mCHH regions plotted against GC content for *Brachypodium distachyon*, *Zea mays*, *Sorghum bicolor*, *Glycine max*, and *Solanum lycopersicum*. (**C**) Average cytosine methylation levels in the CHG context of CHG-DMRs between *Os-dcc* and *Os-ddccc* in *Os-dcc*, *Os-ddcc* and *Os-ddccc* mutants. (**D**) Average cytosine methylation levels in the CHH context of CHH-DMRs between *Os-dcc* and *Os-ddccc* in *Os-dcc*, *Os-ddcc* and *Os-ddccc* mutants.The data point density plots were calculated using 200bp fixed bins across the genome. The data point density bar indicates the values of two-dimensional kernel density estimation. N: the number of mCHG/mCHH regions. The dashed line (**A** - **D**) locates at 0.5 of GC content, and divides the highly GC-rich regions with GC content 0.5~1.

Parsed Citations

Akalin, A., Kormaksson, M., Li, S., Garrett-Bakelman, F.E., Figueroa, M.E., Melnick, A., and Mason, C.E. (2012). methylKit: a comprehensive R package for the analysis of genome-wide DNA methylation profiles. Genome Biol. 13, R87.
Google Scholar: Author Only Title Only Author and Title

Alexa, A., Rahnenfuhrer, J., and Lengauer, T. (2006). Improved scoring of functional groups from gene expression data by decorrelating GO graph structure. Bioinformatics (Oxford, England) 22, 1600-1607.
Google Scholar: Author Only Title Only Author and Title

Anders, S., Pyl, P.T., and Huber, W. (2015). HTSeq-a Python framework to work with high-throughput sequencing data. Bioinformatics (Oxford, England) 31, 166-169.
Google Scholar: Author Only Title Only Author and Title

Bestor, T.H., and Verdine, G.L. (1994). DNA methyltransferases. Current opinion in cell biology 6, 380-389.
Google Scholar: Author Only Title Only Author and Title

Bewick, A.J., Niederhuth, C.E., Ji, L., Rohr, N.A., Griffin, P.T., Leebens-Mack, J., and Schmitz, R.J. (2017). The evolution of CHROMOMETHYLASES and gene body DNA methylation in plants. Genome biology 18, 65.
Google Scholar: Author Only Title Only Author and Title

Borges, F., and Martienssen, R.A. (2015). The expanding world of small RNAs in plants. Nat. Rev. Mol. Cell Biol. 16, 727-741.
Google Scholar: Author Only Title Only Author and Title

Cao, X., and Jacobsen, S.E. (2002). Locus-specific control of asymmetric and CpNpG methylation by the DRM and CMT3 methyltransferase genes. Proc Natl Acad Sci U S A 99 Suppl 4, 16491-16498.
Google Scholar: Author Only Title Only Author and Title

Cao, X., Aufsatz, W., Zilberman, D., Mette, M.F., Huang, M.S., Matzke, M., and Jacobsen, S.E. (2003). Role of the DRM and CMT3 methyltransferases in RNA-directed DNA methylation. Curr. Biol. 13, 2212-2217.
Google Scholar: Author Only Title Only Author and Title

Chen, K., Wang, Y., Zhang, R., Zhang, H., and Gao, C. (2019). CRISPR/Cas genome editing and precision plant breeding in agriculture. Annu. Rev. Plant Biol. 70, 667-697.
Google Scholar: Author Only Title Only Author and Title

Cheng, C., Tarutani, Y., Miyao, A., Ito, T., Yamazaki, M., Sakai, H., Fukai, E., and Hirochika, H. (2015). Loss of function mutations in the rice chromomethylase OsCMT3a cause a burst of transposition. Plant J. 83, 1069-1081.
Google Scholar: Author Only Title Only Author and Title

Du, J., Johnson, L.M., Jacobsen, S.E., and Patel, D.J. (2015). DNA methylation pathways and their crosstalk with histone methylation. Nat. Rev. Mol. Cell Biol. 16, 519-532.
Google Scholar: Author Only Title Only Author and Title

Du, J., Zhong, X., Bernatavichute, Y.V., Stroud, H., Feng, S., Caro, E., Vashisht, A.A., Terragni, J., Chin, H.G., Tu, A., Hetzel, J., Wohlschlegel, J.A., Pradhan, S., Patel, D.J., and Jacobsen, S.E. (2012). Dual binding of chromomethylase domains to H3K9me2-containing nucleosomes directs DNA methylation in plants. Cell 151, 167-180.
Google Scholar: Author Only Title Only Author and Title

Eichten, S.R., Briskine, R., Song, J., Li, Q., Swanson-Wagner, R., Hermanson, P.J., Waters, A.J., Starr, E., West, P.T., Tiffin, P., Myers, C.L., Vaughn, M.W., and Springer, N.M. (2013). Epigenetic and genetic influences on DNA methylation variation in maize populations. The Plant cell 25, 2783-2797.
Google Scholar: Author Only Title Only Author and Title

Fang, Y., Wang, X., Wang, L., Pan, X., Xiao, J., Wang, X.E., Wu, Y., and Zhang, W. (2016). Functional characterization of open chromatin in bidirectional promoters of rice. Sci Rep 6, 32088.
Google Scholar: Author Only Title Only Author and Title

Gouil, Q., and Baulcombe, D.C. (2016). DNA Methylation Signatures of the Plant Chromomethyltransferases. Plos Genet 12, e1006526.
Google Scholar: Author Only Title Only Author and Title

He, X.J., Chen, T., and Zhu, J.K. (2011). Regulation and function of DNA methylation in plants and animals. Cell Res. 21, 442-465.
Google Scholar: Author Only Title Only Author and Title

He, Y., and Ecker, J.R. (2015). Non-CG Methylation in the Human Genome. Annu Rev Genomics Hum Genet 16, 55-77.
Google Scholar: Author Only Title Only Author and Title

Henderson, I.R., Deleris, A., Wong, W., Zhong, X., Chin, H.G., Horwitz, G.A., Kelly, K.A., Pradhan, S., and Jacobsen, S.E. (2010). The de novo cytosine methyltransferase DRM2 requires intact UBA domains and a catalytically mutated paralog DRM3 during RNA-directed DNA methylation in Arabidopsis thaliana. Plos Genet 6, e1001182.
Google Scholar: Author Only Title Only Author and Title

Hu, L., Li, N., Xu, C., Zhong, S., Lin, X., Yang, J., Zhou, T., Yuliang, A., Wu, Y., Chen, Y.R., Cao, X., Zemach, A., Rustgi, S., von Wettstein,

D., and Liu, B. (2014). Mutation of a major CG methylase in rice causes genome-wide hypomethylation, dysregulated genome expression, and seedling lethality. Proc. Natl. Acad. Sci. USA 111, 10642-10647.
Google Scholar: Author Only Title Only Author and Title

Hu, X., Meng, X., Liu, Q., Li, J., and Wang, K. (2018). Increasing the efficiency of CRISPR-Cas9-VQR precise genome editing in rice. Plant Biotechnol. J. 16, 292-297.
Google Scholar: Author Only Title Only Author and Title

Huala, E., Dickerman, A.W., Garcia-Hernandez, M., Weems, D., Reiser, L., LaFond, F., Hanley, D., Kiphart, D., Zhuang, M., Huang, W., Mueller, L.A., Bhattacharyya, D., Bhaya, D., Sobral, B.W., Beavis, W., Meinke, D.W., Town, C.D., Somerville, C., and Rhee, S.Y. (2001). The Arabidopsis Information Resource (TAIR): a comprehensive database and web-based information retrieval, analysis, and visualization system for a model plant. Nucleic Acids Res. 29, 102-105.
Google Scholar: Author Only Title Only Author and Title

Jiao, Y., Peluso, P., Shi, J., Liang, T., Stitzer, M.C., Wang, B., Campbell, M.S., Stein, J.C., Wei, X., Chin, C.S., Guill, K., Regulski, M., Kumari, S., Olson, A., Gent, J., Schneider, K.L., Wolfgruber, T.K., May, M.R., Springer, N.M., Antoniou, E., McCombie, W.R., Presting, G.G., McMullen, M., Ross-Ibarra, J., Dawe, R.K., Hastie, A., Rank, D.R., and Ware, D. (2017). Improved maize reference genome with single-molecule technologies. Nature 546, 524-527.
Google Scholar: Author Only Title Only Author and Title

Jullien, P.E., Susaki, D., Yelagandula, R., Higashiyama, T., and Berger, F. (2012). DNA methylation dynamics during sexual reproduction in Arabidopsis thaliana. Curr. Biol. 22, 1825-1830.
Google Scholar: Author Only Title Only Author and Title

Kawahara, Y., de la Bastide, M., Hamilton, J.P., Kanamori, H., McCombie, W.R., Ouyang, S., Schwartz, D.C., Tanaka, T., Wu, J., Zhou, S., Childs, K.L., Davidson, R.M., Lin, H., Quesada-Ocampo, L., Vaillancourt, B., Sakai, H., Lee, S.S., Kim, J., Numa, H., Itoh, T., Buell, C.R., and Matsumoto, T. (2013). Improvement of the Oryza sativa Nipponbare reference genome using next generation sequence and optical map data. Rice 6, 4.
Google Scholar: Author Only Title Only Author and Title

Kim, D., Langmead, B., and Salzberg, S.L. (2015). HISAT: a fast spliced aligner with low memory requirements. Nat. Methods 12, 357-360.
Google Scholar: Author Only Title Only Author and Title

Knott, G.J., and Doudna, J.A. (2018). CRISPR-Cas guides the future of genetic engineering. Science 361, 866-869.
Google Scholar: Author Only Title Only Author and Title

Lang, Z., Lei, M., Wang, X., Tang, K., Miki, D., Zhang, H., Mangrauthia, S.K., Liu, W., Nie, W., Ma, G., Yan, J., Duan, C.G., Hsu, C.C., Wang, C., Tao, W.A., Gong, Z., and Zhu, J.K. (2015). The methyl-CpG-binding protein MBD7 facilitates active DNA demethylation to limit DNA hyper-methylation and transcriptional gene silencing. Mol Cell 57, 971-983.
Google Scholar: Author Only Title Only Author and Title

Langmead, B., and Salzberg, S.L. (2012). Fast gapped-read alignment with Bowtie 2. Nature methods 9, 357-359.
Google Scholar: Author Only Title Only Author and Title

Langmead, B., Trapnell, C., Pop, M., and Salzberg, S.L. (2009). Ultrafast and memory-efficient alignment of short DNA sequences to the human genome. Genome Biol. 10, R25.
Google Scholar: Author Only Title Only Author and Title

Law, J.A., and Jacobsen, S.E. (2010). Establishing, maintaining and modifying DNA methylation patterns in plants and animals. Nature Rev. Genet. 11, 204-220.
Google Scholar: Author Only Title Only Author and Title

Li, D., Palanca, A.M.S., Won, S.Y., Gao, L., Feng, Y., Vashisht, A.A., Liu, L., Zhao, Y., Liu, X., Wu, X., Li, S., Le, B., Kim, Y.J., Yang, G., Li, S., Liu, J., Wohlschlegel, J.A., Guo, H., Mo, B., Chen, X., and Law, J.A. (2017a). The MBD7 complex promotes expression of methylated transgenes without significantly altering their methylation status. Elife 6.
Google Scholar: Author Only Title Only Author and Title

Li, J., Sun, Y., Du, J., Zhao, Y., and Xia, L. (2017b). Generation of targeted point mutations in rice by a modified CRISPR/Cas9 system. Mol. Plant 10, 526-529.
Google Scholar: Author Only Title Only Author and Title

Li, Q., Gent, J.I., Zynda, G., Song, J., Makarevitch, I., Hirsch, C.D., Hirsch, C.N., Dawe, R.K., Madzima, T.F., McGinnis, K.M., Lisch, D., Schmitz, R.J., Vaughn, M.W., and Springer, N.M. (2015). RNA-directed DNA methylation enforces boundaries between heterochromatin and euchromatin in the maize genome. Proc Natl Acad Sci U S A 112, 14728-14733.
Google Scholar: Author Only Title Only Author and Title

Li, Q., Eichten, S.R., Hermanson, P.J., Zaunbrecher, V.M., Song, J., Wendt, J., Rosenbaum, H., Madzima, T.F., Sloan, A.E., Huang, J., Burgess, D.L., Richmond, T.A., McGinnis, K.M., Meeley, R.B., Danilevskaya, O.N., Vaughn, M.W., Kaeppler, S.M., Jeddeloh, J.A., and Springer, N.M. (2014). Genetic perturbation of the maize methylome. The Plant cell 26, 4602-4616.
Google Scholar: Author Only Title Only Author and Title

Lin, J.Y., Le, B.H., Chen, M., Henry, K.F., Hur, J., Hsieh, T.F., Chen, P.Y., Pelletier, J.M., Pellegrini, M., Fischer, R.L., Harada, J.J., and Goldberg, R.B. (2017). Similarity between soybean and Arabidopsis seed methylomes and loss of non-CG methylation does not affect

seed development. Proc. Natl. Acad. Sci. USA 114, E9730-e9739.
Google Scholar: Author Only Title Only Author and Title

Lister, R., O'Malley, R.C., Tonti-Filippini, J., Gregory, B.D., Berry, C.C., Millar, A.H., and Ecker, J.R. (2008). Highly integrated single-base resolution maps of the epigenome in Arabidopsis. Cell 133, 523-536.
Google Scholar: Author Only Title Only Author and Title

Lister, R., Pelizzola, M., Dowen, R.H., Hawkins, R.D., Hon, G., Tonti-Filippini, J., Nery, J.R., Lee, L., Ye, Z., Ngo, Q.M., Edsall, L., Antosiewicz-Bourget, J., Stewart, R., Ruotti, V., Millar, A.H., Thomson, J.A., Ren, B., and Ecker, J.R. (2009). Human DNA methylomes at base resolution show widespread epigenomic differences. Nature 462, 315-322.
Google Scholar: Author Only Title Only Author and Title

Liu, Q., Wang, C., Jiao, X., Zhang, H., Song, L., Li, Y., Gao, C., and Wang, K. (2019). Hi-TOM: a platform for high-throughput tracking of mutations induced by CRISPR/Cas systems. Sci. China C Life Sci. 62, 1-7.
Google Scholar: Author Only Title Only Author and Title

Long, J., Liu, J., Xia, A., Springer, N.M., and He, Y. (2021). Maize Decrease in DNA methylation 1 targets RNA-directed DNA methylation on active chromatin. The Plant cell.
Google Scholar: Author Only Title Only Author and Title

Love, M.I., Huber, W., and Anders, S. (2014). Moderated estimation of fold change and dispersion for RNA-seq data with DESeq2. Genome Biol. 15, 550.
Google Scholar: Author Only Title Only Author and Title

Martin, M. (2011). Cutadapt removes adapter sequences from high-throughput sequencing reads. EMBnet.journal 17, 10-12.
Google Scholar: Author Only Title Only Author and Title

Matzke, M.A., and Mosher, R.A. (2014). RNA-directed DNA methylation: an epigenetic pathway of increasing complexity. Nature Rev. Genet. 15, 394-408.
Google Scholar: Author Only Title Only Author and Title

McCormick, R.F., Truong, S.K., Sreedasyam, A., Jenkins, J., Shu, S., Sims, D., Kennedy, M., Amirebrahimi, M., Weers, B.D., McKinley, B., Mattison, A., Morishige, D.T., Grimwood, J., Schmutz, J., and Mullet, J.E. (2018). The Sorghum bicolor reference genome: improved assembly, gene annotations, a transcriptome atlas, and signatures of genome organization. Plant J. 93, 338-354.
Google Scholar: Author Only Title Only Author and Title

Moritoh, S., Eun, C.H., Ono, A., Asao, H., Okano, Y., Yamaguchi, K., Shimatani, Z., Koizumi, A., and Terada, R. (2012). Targeted disruption of an orthologue of DOMAINS REARRANGED METHYLASE 2, OsDRM2, impairs the growth of rice plants by abnormal DNA methylation. Plant J. 71, 85-98.
Google Scholar: Author Only Title Only Author and Title

Niederhuth, C.E., Bewick, A.J., Ji, L., Alabady, M.S., Kim, K.D., Li, Q., Rohr, N.A., Rambani, A., Burke, J.M., Udall, J.A., Egesi, C., Schmutz, J., Grimwood, J., Jackson, S.A., Springer, N.M., and Schmitz, R.J. (2016). Widespread natural variation of DNA methylation within angiosperms. Genome Biol. 17, 194.
Google Scholar: Author Only Title Only Author and Title

Pertea, M., Kim, D., Pertea, G.M., Leek, J.T., and Salzberg, S.L. (2016). Transcript-level expression analysis of RNA-seq experiments with HISAT, StringTie and Ballgown. Nat. Protoc. 11, 1650-1667.
Google Scholar: Author Only Title Only Author and Title

Ronemus, M.J., Galbiati, M., Ticknor, C., Chen, J., and Dellaporta, S.L. (1996). Demethylation-induced developmental pleiotropy in Arabidopsis. Science 273, 654-657.
Google Scholar: Author Only Title Only Author and Title

Schultz, M.D., Schmitz, R.J., and Ecker, J.R. (2012). 'Leveling' the playing field for analyses of single-base resolution DNA methylomes. Trends in genetics : TIG 28, 583-585.
Google Scholar: Author Only Title Only Author and Title

Schultz, M.D., He, Y., Whitaker, J.W., Hariharan, M., Mukamel, E.A., Leung, D., Rajagopal, N., Nery, J.R., Urich, M.A., Chen, H., Lin, S., Lin, Y., Jung, I., Schmitt, A.D., Selvaraj, S., Ren, B., Sejnowski, T.J., Wang, W., and Ecker, J.R. (2015). Human body epigenome maps reveal noncanonical DNA methylation variation. Nature 523, 212-216.
Google Scholar: Author Only Title Only Author and Title

Sharma, R., Mohan Singh, R.K., Malik, G., Deveshwar, P., Tyagi, A.K., Kapoor, S., and Kapoor, M. (2009). Rice cytosine DNA methyltransferases - gene expression profiling during reproductive development and abiotic stress. FEBS J. 276, 6301-6311.
Google Scholar: Author Only Title Only Author and Title

Shearer, L.A., Anderson, L.K., de Jong, H., Smit, S., Goicoechea, J.L., Roe, B.A., Hua, A., Giovannoni, J.J., and Stack, S.M. (2014). Fluorescence in situ hybridization and optical mapping to correct scaffold arrangement in the tomato genome. G3: Genes | Genomes | Genetics 4, 1395-1405.
Google Scholar: Author Only Title Only Author and Title

Shen, L., Shao, N., Liu, X., and Nestler, E. (2014). ngs.plot: Quick mining and visualization of next-generation sequencing data by

integrating genomic databases. BMC genomics 15, 284.
Google Scholar: Author Only Title Only Author and Title

Smarda, P., Bures, P., Horova, L., Leitch, I.J., Mucina, L., Pacini, E., Tichy, L., Grulich, V., and Rotreklova, O. (2014). Ecological and evolutionary significance of genomic GC content diversity in monocots. Proc. Natl. Acad. Sci. USA 111, E4096-4102.
Google Scholar: Author Only Title Only Author and Title

Song, Q., Jenkins, J., Jia, G., Hyten, D.L., Pantalone, V., Jackson, S.A, Schmutz, J., and Cregan, P.B. (2016). Construction of high resolution genetic linkage maps to improve the soybean genome sequence assembly Glyma1.01. BMC genomics 17, 33.
Google Scholar: Author Only Title Only Author and Title

Song, X., Li, Y., Cao, X., and Qi, Y. (2019). MicroRNAs and their regulatory roles in plant-environment interactions. Annu. Rev. Plant Biol. 70, 489-525.
Google Scholar: Author Only Title Only Author and Title

Stroud, H., Greenberg, M.V., Feng, S., Bernatavichute, Y.V., and Jacobsen, S.E. (2013a). Comprehensive analysis of silencing mutants reveals complex regulation of the Arabidopsis methylome. Cell 152, 352-364.
Google Scholar: Author Only Title Only Author and Title

Stroud, H., Do, T., Du, J., Zhong, X., Feng, S., Johnson, L., Patel, D.J., and Jacobsen, S.E. (2014). Non-CG methylation patterns shape the epigenetic landscape in Arabidopsis. Nature Struct. Mol. Biol. 21, 64-72.
Google Scholar: Author Only Title Only Author and Title

Stroud, H., Ding, B., Simon, S.A., Feng, S., Bellizzi, M., Pellegrini, M., Wang, G.L., Meyers, B.C., and Jacobsen, S.E. (2013b). Plants regenerated from tissue culture contain stable epigenome changes in rice. eLife 2, e00354.
Google Scholar: Author Only Title Only Author and Title

Tan, F., Zhou, C., Zhou, Q., Zhou, S., Yang, W., Zhao, Y., Li, G., and Zhou, D.X. (2016). Analysis of chromatin regulators reveals specific features of rice DNA methylation pathways. Plant Physiol. 171, 2041-2054.
Google Scholar: Author Only Title Only Author and Title

Tatarinova, T.V., Alexandrov, N.N., Bouck, J.B., and Feldmann, K.A. (2010). GC3 biology in corn, rice, sorghum and other grasses. BMC genomics 11, 308.
Google Scholar: Author Only Title Only Author and Title

Thomas, M.F., and Ansel, K.M. (2010). Construction of small RNA cDNA libraries for deep sequencing. Methods in molecular biology (Clifton, N.J.) 667, 93-111.
Google Scholar: Author Only Title Only Author and Title

Turco, G.M., Kajala, K., Kunde-Ramamoorthy, G., Ngan, C.Y., Olson, A., Deshphande, S., Tolkunov, D., Waring, B., Stelpflug, S., Klein, P., Schmutz, J., Kaeppler, S., Ware, D., Wei, C.L., Etchells, J.P., and Brady, S.M. (2017). DNA methylation and gene expression regulation associated with vascularization in Sorghum bicolor. New Phytol. 214, 1213-1229.
Google Scholar: Author Only Title Only Author and Title

Vogel, J.P., Garvin, D.F., Mockler, T.C., Schmutz, J., Rokhsar, D., Bevan, M.W., Barry, K., Lucas, S., Harmon-Smith, M., Lail, K., Tice, H., Schmutz, J., Grimwood, J., McKenzie, N., Bevan, M.W., Huo, N., Gu, Y.Q., Lazo, G.R., Anderson, O.D., Vogel, J.P., You, F.M., Luo, M.-C., Dvorak, J., Wright, J., Febrer, M., Bevan, M.W., Idziak, D., Hasterok, R., Garvin, D.F., Lindquist, E., Wang, M., Fox, S.E., Priest, H.D., Filichkin, S.A, Givan, S.A, Bryant, D.W., Chang, J.H., Mockler, T.C., Wu, H., Wu, W., Hsia, A.-P., Schnable, P.S., Kalyanaraman, A., Barbazuk, B., Michael, T.P., Hazen, S.P., Bragg, J.N., Laudencia-Chingcuanco, D., Vogel, J.P., Garvin, D.F., Weng, Y., McKenzie, N., Bevan, M.W., Haberer, G., Spannagl, M., Mayer, K., Rattei, T., Mitros, T., Rokhsar, D., Lee, S.-J., Rose, J.K.C., Mueller, L.A, York, T.L., Wicker, T., Buchmann, J.P., Tanskanen, J., Schulman, A.H., Gundlach, H., Wright, J., Bevan, M., Costa de Oliveira, A, da C. Maia, L., Belknap, W., Gu, Y.Q., Jiang, N., Lai, J., Zhu, L., Ma, J., Sun, C., Pritham, E., Salse, J., Murat, F., Abrouk, M., Haberer, G., Spannagl, M., Mayer, K., Bruggmann, R., Messing, J., You, F.M., Luo, M.-C., Dvorak, J., Fahlgren, N., Fox, S.E., Sullivan, C.M., Mockler, T.C., Carrington, J.C., Chapman, E.J., May, G.D., Zhai, J., Ganssmann, M., Guna Ranjan Gurazada, S., German, M., Meyers, B.C., Green, P.J., Bragg, J.N., Tyler, L., Wu, J., Gu, Y.Q., Lazo, G.R., Laudencia-Chingcuanco, D., Thomson, J., Vogel, J.P., Hazen, S.P., Chen, S., Scheller, H.V., Harholt, J., Ulvskov, P., Fox, S.E., Filichkin, S.A, Fahlgren, N., Kimbrel, J.A, Chang, J.H., Sullivan, C.M., Chapman, E.J., Carrington, J.C., Mockler, T.C., Bartley, L.E., Cao, P., Jung, K.-H., Sharma, M.K., Vega-Sanchez, M., Ronald, P., Dardick, C.D., De Bodt, S., Verelst, W., Inzé, D., Heese, M., Schnittger, A, Yang, X., Kalluri, U.C., Tuskan, G.A, Hua, Z., Vierstra, R.D., Garvin, D.F., Cui, Y., Ouyang, S., Sun, Q., Liu, Z., Yilmaz, A, Grotewold, E., Sibout, R., Hematy, K., Mouille, G., Höfte, H., Michael, T., Pelloux, J., O'Connor, D., Schnable, J., Rowe, S., Harmon, F., Cass, C.L., Sedbrook, J.C., Byrne, M.E., Walsh, S., Higgins, J., Bevan, M., Li, P., Brutnell, T., Unver, T., Budak, H., Belcram, H., Charles, M., Chalhoub, B., Baxter, I., The International Brachypodium, I., Principal, i., sequencing, D.N.A, assembly, Pseudomolecule, a., sequencing, B.A.C.e., Transcriptome, s., analysis, Gene, a., annotation, Repeats, a., Comparative, g., Small, R.N.A.a., Manual, a., and gene family, a. (2010). Genome sequencing and analysis of the model grass Brachypodium distachyon. Nature 463, 763-768.
Google Scholar: Author Only Title Only Author and Title

Wang, C., Shen, L., Fu, Y., Yan, C., and Wang, K. (2015). A simple CRISPR/Cas9 system for multiplex genome editing in rice. J. Genet. Genom. 42, 703-706.
Google Scholar: Author Only Title Only Author and Title

Xi, Y., and Li, W. (2009). BSMAP: whole genome bisulfite sequence MAPping program. BMC bioinformatics 10, 232.
Google Scholar: Author Only Title Only Author and Title

Xie, W., Barr, C.L., Kim, A., Yue, F., Lee, A.Y., Eubanks, J., Dempster, E.L., and Ren, B. (2012). Base-resolution analyses of sequence and parent-of-origin dependent DNA methylation in the mouse genome. Cell 148, 816-831.
Google Scholar: Author Only Title Only Author and Title

Yamauchi, T., Johzuka-Hisatomi, Y., Terada, R., Nakamura, I., and Iida, S. (2014). The MET1b gene encoding a maintenance DNA methyltransferase is indispensable for normal development in rice. Plant Mol. Biol. 85, 219-232.
Google Scholar: Author Only Title Only Author and Title

Yamauchi, T., Johzuka-Hisatomi, Y., Fukada-Tanaka, S., Terada, R., Nakamura, I., and Iida, S. (2009). Homologous recombination-mediated knock-in targeting of the MET1a gene for a maintenance DNA methyltransferase reproducibly reveals dosage-dependent spatiotemporal gene expression in rice. Plant J. 60, 386-396.
Google Scholar: Author Only Title Only Author and Title

Yu, J., Hu, S., Wang, J., Wong, G.K.-S., Li, S., Liu, B., Deng, Y., Dai, L., Zhou, Y., Zhang, X., Cao, M., Liu, J., Sun, J., Tang, J., Chen, Y., Huang, X., Lin, W., Ye, C., Tong, W., Cong, L., Geng, J., Han, Y., Li, L., Li, W., Hu, G., Huang, X., Li, W., Li, J., Liu, Z., Li, L., Liu, J., Qi, Q., Liu, J., Li, L., Li, T., Wang, X., Lu, H., Wu, T., Zhu, M., Ni, P., Han, H., Dong, W., Ren, X., Feng, X., Cui, P., Li, X., Wang, H., Xu, X., Zhai, W., Xu, Z., Zhang, J., He, S., Zhang, J., Xu, J., Zhang, K., Zheng, X., Dong, J., Zeng, W., Tao, L., Ye, J., Tan, J., Ren, X., Chen, X., He, J., Liu, D., Tian, W., Tian, C., Xia, H., Bao, Q., Li, G., Gao, H., Cao, T., Wang, J., Zhao, W., Li, P., Chen, W., Wang, X., Zhang, Y., Hu, J., Wang, J., Liu, S., Yang, J., Zhang, G., Xiong, Y., Li, Z., Mao, L., Zhou, C., Zhu, Z., Chen, R., Hao, B., Zheng, W., Chen, S., Guo, W., Li, G., Liu, S., Tao, M., Wang, J., Zhu, L., Yuan, L., and Yang, H. (2002). A Draft Sequence of the Rice Genome (*Oryza sativa* L. ssp. *indica*). Science 296, 79-92.
Google Scholar: Author Only Title Only Author and Title

Zemach, A., Kim, M.Y., Hsieh, P.H., Coleman-Derr, D., Eshed-Williams, L., Thao, K., Harmer, S.L., and Zilberman, D. (2013). The Arabidopsis nucleosome remodeler DDM1 allows DNA methyltransferases to access H1-containing heterochromatin. Cell 153, 193-205.
Google Scholar: Author Only Title Only Author and Title

Zhang, H., Lang, Z., and Zhu, J.K. (2018). Dynamics and function of DNA methylation in plants. Nat. Rev. Mol. Cell Biol. 19, 489-506.
Google Scholar: Author Only Title Only Author and Title

Zheng, D., Wang, L., Chen, L., Pan, X., Lin, K., Fang, Y., Wang, X.E., and Zhang, W. (2019). Salt-Responsive Genes are Differentially Regulated at the Chromatin Levels Between Seedlings and Roots in Rice. Plant Cell Physiol 60, 1790-1803.
Google Scholar: Author Only Title Only Author and Title

Zhong, X., Hale, C.J., Nguyen, M., Ausin, I., Groth, M., Hetzel, J., Vashisht, A.A., Henderson, I.R., Wohlschlegel, J.A., and Jacobsen, S.E. (2015). Domains rearranged methyltransferase3 controls DNA methylation and regulates RNA polymerase V transcript abundance in Arabidopsis. Proc Natl Acad Sci U S A 112, 911-916.
Google Scholar: Author Only Title Only Author and Title

Zhou, M., Palanca, A.M.S., and Law, J.A. (2018). Locus-specific control of the de novo DNA methylation pathway in Arabidopsis by the CLASSY family. Nature genetics 50, 865-873.
Google Scholar: Author Only Title Only Author and Title